Ebrahimpoor Gorji, Ali; Laakso, Juho-Pekka; Alopaeus, Ville; Uusi-Kyyny, Petri

Towards the prediction of infinite dilution activity coefficient (IDAC) of methanol in ionic liquids (ILs) using QSPR-based COSMO descriptors: Considering temperature effect using machine learning

Published in:
Fuel

DOI:
10.1016/j.fuel.2025.134674

E-pub ahead of print: 15/06/2025

Document Version
Publisher's PDF, also known as Version of record

Fuel 390 (2025) 134674

Contents lists available at ScienceDirect

Fuel

journal homepage: www.elsevier.com/locate/fuel

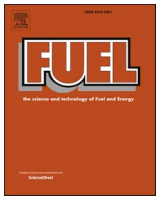

Full Length Article

Towards the prediction of infinite dilution activity coefficient (IDAC) of methanol in ionic liquids (ILs) using QSPR-based COSMO descriptors: Considering temperature effect using machine learning

Ali Ebrahimpoor Gorji, Juho-Pekka Laakso, Ville Alopaeus *, Petri Uusi-Kyyny

Aalto University, School of Chemical Technology, Department of Chemical and Metallurgical Engineering, Research Group of Chemical Engineering, P.O. Box 16100 FI-00076 Aalto, Finland

ARTICLE INFO

Keywords:
IDAC of Methanol
QSPR
Ionic Liquids
Prediction
van't Hoff equation
Temperature effects

ABSTRACT

In this study, the 'Quantitative Structure-Activity/Property Relationship' (QSAR/QSPR) approach has been applied for the prediction of infinite dilution activity coefficient (IDAC) of Methanol (MeOH) in Ionic Liquids (ILs) using an extensive dataset. A new predictive QSPR model including novel molecular descriptors, called 'COSMO-RS descriptors', has been developed for the first time. In this study, the dataset was divided to a training set for the development of models, and a validation set for external validation. According to the obtained results of statistical parameters ($R^2 = 0.92$ and $Q^2_{LOO\text{-}CV} = 0.91$), the predictive capability of the developed QSPR model was acceptable for training set. Regarding the external validation, other statistical parameters such as AAD = 0.2034 and RMSE = 0.2926 were also satisfactory for validation set. While the values of IDAC increase or decrease with increasing temperature, the QSPR model based on the van't Hoff equation takes into account the 'negative' and 'positive' effects of temperature on the IDAC of MeOH in ILs well, depending on the nature of ILs. It was also shown that the IDAC value in some new ILs, which had not been experimentally studied before, can be predicted using QSPR model. These predicted data can be considered as 'Pseudo Experimental data' for future efforts.

1. Introduction

Methanol (MeOH) as one of the main alcoholic compounds and Ionic Liquids (ILs) are simultaneously present in various chemical processes such as alkylation of hydroquinone [1] and synthesis of dimethyl carbonate (DMC) [2,3]. For instance, CO_2 and methanol can be directly converted into DMC, in the presence of ILs. ILs have emerged as promising solvents in different chemical processes due to some unique and intrinsic characteristics of ILs, such as high selectivity, high degradation temperature, low vapor pressure and low flammability [4]. They are a low temperature molten salt composed of 'bulky asymmetric organic cation' and 'inorganic or organic anion'. According to the nature of cations, ILs are often categorized as Pyridinium, Imidazolium, Ammonium, Phosphonium etc. However, a molecular insight of their interactions with other components like MeOH is still required. For this reason, a binary mixture including ILs and MeOH is gaining more visibility in the chemical field.

Infinite Dilution Activity Coefficient (IDAC) as one of the important thermodynamic properties has been frequently studied in the binary mixture of IL and MeOH. Since, IDAC can provide helpful information on chemical potential and enthalpy change, it is a good criterion for finding the most appropriate IL with the highest or lowest affinity into the MeOH, with respect to the chemical applications [5]. IDAC values show the interaction between solvent and solute [6]. In other words, the higher solute–solvent interaction, the lower activity coefficient and vice versa. The structural effects of anion and cation of IL on the IDAC of MeOH have been investigated experimentally and computationally by researchers.

There are many well-known methods for the determination of IDAC of compounds in the liquid phase using dilution, such as Gas-Liquid Chromatography (GLC), and Vapor-Liquid Equilibria (VLE) methods [7]. Domanska et al. [8,9] as one of the most active research groups in this field, measured the values of IDAC of MeOH (i.e., γ^{∞}_{MeOH}) in [HMIM][SCN] and [1B1MPyrro][CF_3SO_3] at eight temperatures (i.e., 298, 308, 318, 328, 338, 348, 358, and 368 K). In the last few years, Mutelet et al. [10,11] have experimentally reported the values of IDAC of MeOH in

* Corresponding author.
E-mail address: ville.alopaeus@aalto.fi (V. Alopaeus).

https://doi.org/10.1016/j.fuel.2025.134674
Received 10 June 2024; Received in revised form 2 December 2024; Accepted 9 February 2025
Available online 17 February 2025

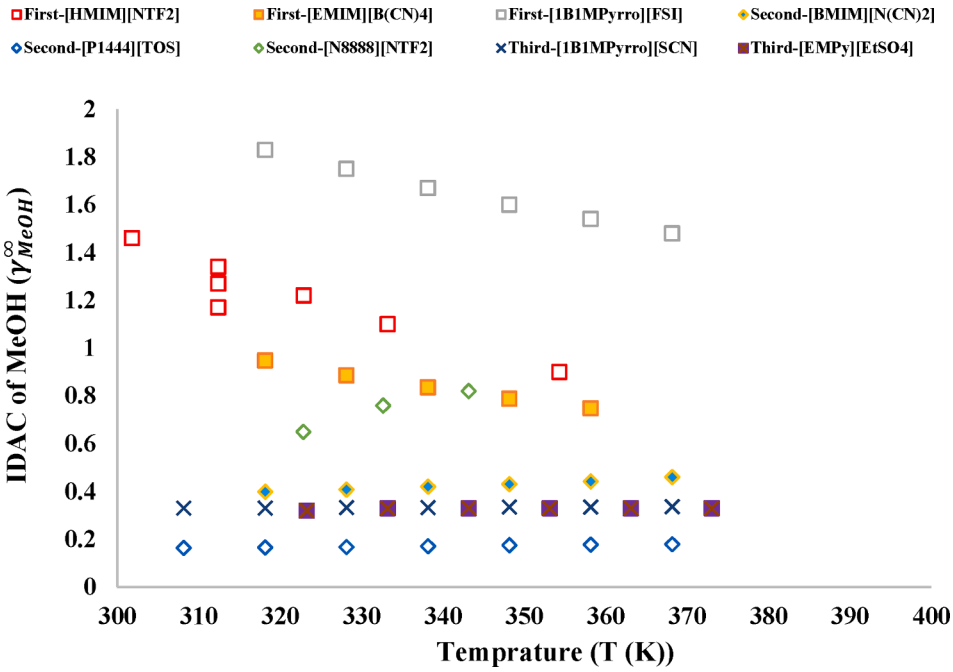

Fig. 1. Examples of ILs from each group with different dependencies to temperature [22,24,29,33,40,50,54,127].

other ILs with constant anion (i.e., [NTF_2]) such as [BzMIM][NTF_2] and [COC2 Py][NTF_2] at six temperatures (i.e., 323, 333, 343, 353, 363, and 373 K). However, there are many experimental works including the large number of cation and anion structural variations, but with an estimation of 10^{18} potential ILs [5], determining of IDAC values for all these binary mixtures (i.e., IL + MeOH) is not practically possible. Hence, the reliable predictive methods are of utmost importance.

Thangarajoo et al. [5] used Group Contribution Method (GCM) for the prediction of IDAC of MeOH in ILs. Due to lack of modeling results for IL-MeOH system, they made comparison GCM's results with Quantitative Structure-Property (or Activity) Relationship (QSPR/QSAR) approach's results of Gonfa et al. [12] which were obtained for IL-Water system. According to this comparison, GCM showed a better performance for prediction of IDAC of solute (MeOH) in ILs in comparison with QSPR/QSAR approach. Gonfa et al. [12], suggested the following multilinear regression QSAR model for the prediction of IDAC of water in ILs (Eq. (1)):

$$ln(\gamma_W^{\infty}) = a_1 S_1^{Cat} + a_2 S_2^{Cat} + a_3 S_3^{Cat} + a_4 S_4^{Cat} + a_5 S_5^{Ani} + a_6 S_6^{Ani} + a_7 S_7^{Ani} + a_8 S_8^{Ani} + \frac{a_9}{T} + a_{10} \quad (1)$$

where, a_1 to a_8 are the adjustable parameters to consider the effect of structural variations (i.e., cation and anion), and a_9 is an adjustable parameter for 1/T to consider the effect of temperature on the IDAC of water in the ILs, according to van't Hoff equation. They divided the sigma profile of each cation and anion into 4 regions. In other words, the occupied areas of each region considered as COSMO-RS numerical molecular descriptors, called 'S_1^{Cat}, S_2^{Cat}, S_3^{Cat}, S_4^{Cat},' and 'S_5^{Ani}, S_6^{Ani}, S_7^{Ani}, S_8^{Ani}'. In former study by Gonfa et al. [13], it has been demonstrated that COSMO-RS model as a direct predictive tool overestimates the IDAC values of water in ILs. For this reason, they tried to develop a new predictive model like Eq. (1). As it is clear, suggested model by Gonfa et al. [12] does not predict temperature dependency for all kinds of ILs well. Because such model always has a constant adjustable parameter ('with positive or negative sign') for '1/T' variable (i.e., a_9). It means that such model cannot distinguish the effect of temperature on the IDAC of MeOH in different ILs. Although the IDAC values of either methanol or water in majority of ILs decrease with an increase in temperature [14], there are some ILs that their IDAC values increase or stay almost constant [5]. For this reason, Gonfa et al [12] presented other QSAR models for IDAC of water in ILs at fixed temperatures.

Thangarajoo et al. [5] considered the effect of temperature on the prediction of IDAC of MeOH in ILs, and applied Gonfa's model with two modifications: they used new independent variables like functional group descriptors instead of COSMO-RS descriptors, and the coefficients of temperature variables (i.e., $\sum B$ and $\sum C$) were set as functions of the molecular descriptors for the first time. They used a small dataset including 158 datapoints and 36 unique ILs (20 cations and 11 anions) for training and validation models. According to the proposed model by Thangarajoo et al. [5] in Eq. (2), the values of molecular descriptors of '1/T and $1/T^{2}$' (i.e., $\sum B$ and $\sum C$) vary with respect to the nature of ILs. There were only three ILs that their experimental values increased with increasing temperature. The $\sum B$ and $\sum C$ descriptors of one of them such as [C_2OHMIM] [FAP], varied in such a way that the GCM-based model predicted decreasing IDAC values with increasing temperature. It seems that a predictive model with considering the effect of temperature for prediction of IDAC of MeOH in large number of ILs with high structural variations of cation and anion is still missing.

$$ln(\gamma_{MeOH}^{\infty}) = \sum A + \frac{\sum B}{T} + \frac{\sum C}{T^2} \quad (2)$$

Thangarajoo et al. [5] evaluated the prediction capability of model using R^2 and AARD% statistical parameters. As AARD% parameter describes relative deviation, datapoints with a low absolute value (i.e., between −0.1 to + 0.1), tend to increase AARD% significantly. In the dataset of Thangarajoo et al. [5], the number of data points with a relatively low absolute value was low which affect the reported AARD% values.

The (QSPR/QSAR) approach as one of the robust Machine Learning (ML) methods is commonly used to make quantitative and qualitative correlation between ILs and their specific properties [15–18]. Unlike the Gonfa et al. [12] and Thangarajoo et al. [5] studies, molecular variables (i.e., descriptors) selection from the descriptors pool has been performed in this QSPR/QSAR study. Therefore, it is possible to design and/or develop new ILs using the QSPR method for different applications. Up to now, no researchers have applied the QSPR/QSAR approach for prediction of IDAC of MeOH in ILs with a large variety of cation and anion structures at a wide range of temperatures. It is the first time that this approach has been applied in the well-known software called 'QSARINS'

Table 1
Studied ILs in different binary systems (i.e., IL + MeOH) with their ranges of temperature and experimental values as well as statistical parameters.

Mixture IL/MeOH	Temperature range (K)	Range of Ln (IDAC $_{Exp}$)	AARD %	AAD	Refs
[HMIM][NTF2]	301–354	(0.378)–(−0.105)	40.5	0.055	[22]
[HMIM][NTF2]	293–353	(0.431)–(−0.072)	62.5	0.055	[23]
[1B4MPy][SCN]	298–368	(−0.975)–(−1.084)	19.9	0.2041	[24]
[1B1MPyrro][SCN]	298–368	(−1.111)–(−1.090)	21	0.2335	[24]
[BMIM][SCN]	298–368	(−0.877)–(−0.962)	21.5	0.2	[25]
[EMIM] [SCN]	**298–368**	**(−0.707)–(−0.778)**	**5.73**	**0.042**	[26]
[BMIM][CF3SO3]	298–368	(−0.305)–(−0.596)	6.42	0.0277	[27]
[Et3S][NTF2]	298–368	(0.482)–(−0.067)	34.4	0.076	[28]
[1B4MPy][NFT2]	298–368	(0.425)–(−0.132)	29	0.039	[6]
[P1444][TOS]	298–368	(−1.783)–(−1.720)	12	0.2138	[29]
[HMIM][SCN]	298–368	(−0.631)–(−0.740)	18	0.1246	[8]
[1B1MPyrro][CF3SO3]	298–368	(−0.332)–(−0.610)	17.7	0.082	[9]
[P66614][BF4]	313–353	(−0.601)–(−0.763)	23.4	0.1602	[30]
[P66614][PF6]	313–363	(0.760)–(−0.126)	64.6	0.2909	[31]
[C10MIM] [B(CN)4]	**318–378**	**(−0.191)–(−0.522)**	**25.67**	**0.0928**	[32]
[EMIM] [B(CN)4]	**298–358**	**(0.095)–(−0.290)**	**67**	**0.087**	[33]
[OMIM][NO3]	303–363	(−1.347)–(−1.514)	16.8	0.24	[34]
[BMIM][NO3]	303–363	(−1.133)–(−1.197)	7.84	0.0912	[35]
[HydEMIM][BF4]	303–363	(0.028)–(−0.223)	372	0.2639	[36]
[N-C3OHPy][NTF2]	318–378	(−0.139)–(−0.352)	235	0.5246	[37]
[BMIM][CLO4]	303–323	(0.067)–(0.048)	1118	0.6374	[38]
[OMIM][MDEGSO4]	288–313	(−0.820)–(−0.967)	29.5	0.2655	[39]
[N2228] [FSI]	**318–368**	**(0.524)–(0.300)**	**44.4**	**0.1702**	[40]
[1B1MPyrro][FSI]	**318–368**	**(0.604)–(0.392)**	**23.5**	**0.1085**	[40]
[EMIM][MESO3]	**308–358**	**(−1.500)–(−1.452)**	**8.8**	**0.1305**	[41]
[1B1MPyrro][C(CN)3]	318–358	(−0.358)–(−0.499)	9.63	0.0395	[42]
[1M1C3Piper][NTF2]	308–358	(0.476)–(0.076)	14.4	0.044	[43]
[C12MIM][NTF2]	318–358	(0.254)–(0.048)	153	0.1607	[44]
[1B1MPyrro] [B(CN)4]	**328–368**	**(−0.092)–(−0.324)**	**28**	**0.0408**	[45]
[HMIM] [B(CN)4]	**318–368**	**(−0.177)–(−0.457)**	**50**	**0.1489**	[46]
[1B1MPyrro][FAP]	318–368	(0.943)–(0.371)	62	0.3843	[47]
[N1112OH][NTF2]	318–368	(−0.149)–(−0.167)	152	0.2465	[48]
[1E1MPyrro][Lac]	358–408	(−2.453)–(−1.987)	12.2	0.2803	[49]
[BMIM][N(CN)2]	318–368	(−0.918)–(−0.776)	13.43	0.1183	[50]
[N-C3OHPy][N(CN)2]	318–368	(−0.382)–(−0.310)	80	0.2722	[51]
[EMMor][N(CN)2]	318–368	(−0.482)–(−0.379)	83	0.3479	[52]
[P4444][NTF2]	358–408	(0.246)–(0.058)	169	0.1972	[53]
[EMPy][EtSO4]	323–373	(−1.139)–(−1.108)	18.3	0.2047	[54]
[BMIM][CF3SO3]	313–363	(−0.393)–(−0.486)	8.62	0.038	[55]
[EMIM] [EtSO4]	**303–353**	**(−0.621)–(−1.081)**	**13.7**	**0.123**	[56]
[EMIM] [C(CN)3]	**318–368**	**(−0.223)–(−0.282)**	**21.22**	**0.056**	[57]
[N-C3OHMIM][N(CN)2]	318–368	(−0.462)–(−0.371)	25.6	0.1012	[58]
[N-C3OHMMor][N(CN)2]	318–368	(−0.283)–(−0.234)	147.5	0.3716	[58]
[1B4MPy][C(CN)3]	318–368	(−0.410)–(−0.544)	22.5	0.1044	[59]
[BMIM][C(CN)3]	318–368	(−0.314)–(−0.462)	28.6	0.1062	[59]
[COC2MPyrro][NTF2]	318–368	(0.314)–(−0.028)	173	0.0964	[60]
[COC2MMor][NTF2]	318–368	(0.246)–(−0.108)	228	0.2213	[61]
[COC2MPip][NTF2]	318–368	(0.314)–(−0.059)	150.4	0.1545	[62]
[COC2MPip][FAP]	318–368	(0.746)–(0.398)	12	0.0667	[63]
[HydEMIM][FAP]	318–368	(−0.372)–(−0.307)	116.7	0.4	[64]
[COC2MPyrro][FAP]	318–368	(0.832)–(0.463)	30.5	0.19	[65]
[COC2 N112][FAP]	318–368	(0.708)–(0.418)	42.65	0.2278	[66]
[HMIM][NTF2]	298–348	(0.412)–(−0.020)	89.3	0.0389	[67]
[CNMe(M)2iPAm][NTF2]	313–363	(0.358)–(0.038)	177.2	0.1877	[68]
[BzMIM][NTF2]	323–373	(0.357)–(−0.067)	75.3	0.0645	[10]
[COC2 Py][NTF2]	323–373	(0.908)–(0.598)	64.22	0.47	[11]
[OMIM][PF6]	313–333	(0.570)–(0.405)	11.5	0.0504	[69]
[1B1MPip][NTF2]	308–358	(0.425)–(0.019)	24.33	0.0561	[70]
[1H1MPip][NTF2]	308–348	(0.412)–(0.076)	52.7	0.107	[71]
[1M1C5Pip][NTF2]	308–348	(0.371)–(0.067)	25.86	0.0479	[71]
[1B1MPyrro][FSI]	323–373	(0.494)–(0.131)	23.12	0.0519	[72]
[1M1C3Pyrro][FSI]	**323–373**	**(0.444)–(0.104)**	**69.67**	**0.144**	[72]
[EMIM] [FSI]	**323–373**	**(0.457)–(0.067)**	**143.66**	**0.2218**	[72]
[1M1C3Pip][FSI]	**323–373**	**(0.553)–(0.165)**	**55.27**	**0.1503**	[72]
[P66614][Cl]	363–413	(−3.411)–(−2.995)	18	0.5833	[73]
[COC2MMor][FAP]	318–368	(0.530)–(0.262)	28.4	0.1106	[74]
[EMIM] [FAP]	**318–368**	**(0.806)–(0.476)**	**42.3**	**0.2598**	[75]
[N-C3OH MMor][NTF2]	318–368	(−0.056)–(−0.136)	460	0.3883	[76]
[C10C10 MIM][N(CN)2]	358–408	(−1.111)–(−1.024)	11.9	0.1247	[77]
[Epy][NTF2]	302–353	(0.641)–(0.122)	36.64	0.141	[78]
[C5Py][NTF2]	302–353	(0.470)–(−0.061)	67.18	0.0711	[78]
[BPy][NTF2]	302–353	(0.693)–(0.113)	30.4	0.138	[78]

(*continued on next page*)

Table 1 (*continued*)

Mixture IL/MeOH	Temperature range (K)	Range of Ln (IDAC $_{Exp}$)	AARD %	AAD	Refs
[HMIM][Cl]	313–363	(−1.924)–(−2.071)	16.33	0.3255	[79]
[HydEMIM][PF6]	303–353	(0.438)–(0.165)	12	0.03	[80]
[C10 MIM][NTF2]	**313–363**	**(0.451)–(0.246)**	**95.2**	**0.3109**	[81]
[Quin6][NTF2]	313–353	(0.413)–(0.196)	52.3	0.1396	[82]
[Quin8][NTF2]	313–343	(0.349)–(0.101)	42.3	0.0838	[82]
[1B1MPyrro][N(CN)2]	318–353	(−1.067)–(−1.055)	19.5	0.208	[83]
[1B1MPyrro][BOB]	333–363	(0.239)–(0.048)	7	0.0092	[84]
[1B1MPyrro][B(CN)4]	333–353	(−0.071)–(−0.185)	93.3	0.101	[84]
[EMIM][MeSO3]	**323–353**	**(−1.431)–(−1.398)**	**4.26**	**0.0605**	[85]
[EMIM] [B(CN)4]	**323–353**	**(−0.116)–(−0.281)**	**64.11**	**0.1167**	[86]
[EMIM] [NTF2]	**303–318**	**(−0.083)–(−0.186)**	**428**	**0.493**	[87]
[1B1MPip][SCN]	318–358	(−1.005)–(−0.986)	18.3	0.1825	[88]
[C8-isoquinolinium][NTF2]	328–368	(0.246)–(−0.087)	228	0.2547	[89]
[1B1MPyrro][N(CN)2]	313–373	(−1.090)–(−1.041)	17.9	0.1938	[90]
[C6-isoquinolinium][SCN]	328–368	(−0.964)–(−0.994)	7.82	0.0768	[91]
[N-C3OH MIM][SCN]	318–358	(−0.331)–(−0.423)	34.8	0.1314	[92]
[C6Py][Br]	333–373	(−1.788)–(−1.845)	7.71	0.1399	[93]
[1B3M Py][CF3SO3]	318–358	(−0.443)–(−0.596)	7	0.036	[94]
[COC2 MPyrro][FAP]	323–353	(0.774)–(0.470)	21.9	0.1375	[95]
[HydEMIM][FAP]	323–353	(−0.362)–(−0.410)	123.9	0.4748	[95]
[Hyd EM Pyrro][MMPO4]	328–368	(−2.525)–(−2.273)	9.5	0.2244	[96]
[BMIM][NTF2]	313–353	(0.231)–(0.029)	141.7	0.1068	[97]
[EMIM] [NO3]	**318–353**	**(−0.572)–(−0.612)**	**83.9**	**0.498**	[98]
[BMIM][MeSO3]	343–383	(−1.171)–(−0.994)	28	0.2958	[99]
[EMIM] [EtSO4]	**312–354**	**(−0.891)–(−1.021)**	**14.9**	**0.1407**	[100]
[P66614][Bis (M) 3 C5 Phos]	363–403	(−3.772)–(−3.381)	8.5	0.3086	[73]
[EMIM] [FAP]	**313–353**	**(0.974)–(0.412)**	**34.9**	**0.2509**	[101]
[EMIM] [B(CN)4]	**303–343**	**(0.122)–(−0.162)**	**32.5**	**0.0249**	[102]
[HMIM][BOB]	308–337	(0.463)–(0.131)	32.8	0.0578	[103]
[BMIM][BOB]	307–347	(0.662)–(0.165)	23.64	0.0798	[103]
[1M3C3 IM][Br]	323–363	(−2.189)–(−2.282)	17.9	0.4026	[104]
[BMIM][BF4]	303–343	(−0.207)–(−0.636)	107.3	0.4262	[105]
[EMIM][MDEGSO4]	**308–333**	**(−0.941)–(−0.996)**	**16.65**	**0.1604**	[106]
[EMIM] [C8SO4]	**318–358**	**(−1.609)–(−1.714)**	**48.62**	**0.8072**	[107]
[OMIM][PF6]	343–373	(−0.150)–(−0.162)	301	0.4693	[108]
[BMIM][PF6]	293–353	(0.951)–(0.307)	15.51	0.0636	[23]

Table 1 (*continued*)

Mixture IL/MeOH	Temperature range (K)	Range of Ln (IDAC $_{Exp}$)	AARD %	AAD	Refs
[BMIM][MeSO4]	**298–353**	**(−0.941)–(−0.967)**	**28.5**	**0.2893**	[23]
[EMIM][H2SO4]	**323–353**	**(−2.441)–(−3.194)**	**32.15**	**0.9073**	[56]
[1B4M Py][BF4]	313–343	(0.075)–(−0.176)	78.6	0.0637	[109]
[EMIM] [NTF2]	**313–343**	**(0.123)–(−0.136)**	**343**	**0.2488**	[110]
[E MM IM][NTF2]	313–343	(0.378)–(0.073)	27.8	0.0712	[110]
[N4111][NTF2]	303–333	(0.438)–(0.139)	16.3	0.0522	[111]
[P14666][N(CN)2]	313–343	(−1.184)–(−1.018)	9.71	0.1026	[112]
[P66614][Bis (M) 3 C5 Phos]	313–343	(−3.506)–(−2.813)	11.36	0.3366	[113]
[Epy][NTF2]	303–323	(0.262)–(0.104)	86.9	0.1381	[114]
[1,3 MMIM][MeSO4]	**303–333**	**(−0.562)–(−0.597)**	**35.16**	**0.2043**	[114]
[HMIM][NTF2]	303–323	(0.262)–(0.095)	66	0.0932	[115]
[OMIM][NTF2]	303–333	(0.207)–(−0.040)	251	0.1267	[115]
[N-C3OH MMor][C(CN)3]	328–358	(−0.149)–(−0.252)	22.55	0.0424	[116]
[EMIM] [NTF2]	**293–323**	**(0.431)–(0.190)**	**26.82**	**0.0719**	[117]
[P66614][NTF2]	303–318	(0.231)–(0.207)	166.7	0.357	[118]
[BMIM][Cl]	398–428	(−1.857)–(−1.655)	23.8	0.4157	[119]
[BMIM][(Me)2PO4]	398–428	(−2.333)–(−2.079)	4.77	0.102	[119]
[3 M 1C14 IM][BF4]	393–433	(−0.426)–(−0.652)	9	0.0443	[120]
[C12 3 M IM][BF4]	323–338	(0.058)–(−0.054)	445	0.2516	[120]
[3 M 1C14 IM][BF4]	358–388	(−0.089)–(−0.257)	189	0.2626	[120]
[CyC3 MIM][N(CN)2]	328–358	(−0.592)–(−0.627)	7.7	0.0475	[121]
[BMIM][BF4]	303–332	(0.198)–(0.165)	88.6	0.1655	[122]
[BMIM][Cl]	323–353	(−2.302)–(−2.162)	1.55	0.0344	[97]
[1,3 BB IM][Br]	333–363	(−1.469)–(−1.427)	25.2	0.3674	[99]
[BMIM][PF6]	343–373	(0.936)–(0.832)	53.6	0.4732	[123]
[P66614][NTF2]	313–373	(0.079)–(−0.147)	478	0.2661	[124]
[1E 2,3MM IM][NTF2]	313–344	(0.378)–(0.073)	30.6	0.0749	[125]
[1B4M Py][BF4]	313–343	(0.075)–(−0.176)	78.58	0.0637	[125]
[N101011][ClO4]	308–353	(−0.805)–(−0.898)	13.91	0.1225	[126]
[N101011][BF4]	308–353	(−1.224)–(−1.117)	67.38	0.8178	[126]
[N1118][NTF2]	322–343	(−0.083)–(−0.210)	148.9	0.2309	[127]
[N8888][NTF2]	322–343	(−0.430)–(−0.198)	42.5	0.1565	[127]
[N4441][NTF2]	322–343	(−0.040)–(−0.127)	361	0.3432	[127]
[P66614][NTF2]	308–318	(−0.059)–(−0.042)	220	0.1043	[128]
[OMIM][BF4]	303–343	(0.086)–(−0.162)	72	0.0609	[129]
[EMIM] [BF4]	**303–343**	**(−0.843)–(−0.867)**	**99**	**0.8435**	[129]
[HMIM[]BF4]	303–323	(0.173)–(0.076)	147	0.1567	[129]

(*continued on next page*)

Table 1 (*continued*)

Mixture IL/MeOH	Temperature range (K)	Range of Ln (IDAC $_{Exp}$)	AARD %	AAD	Refs
[P66614][FAP]	308–318	(0.207)–(0.131)	44.95	0.0732	[130]
[HMIM][PF6]	298–323	(0.662)–(0.364)	36.64	0.1628	[131]
[BMIM] [C8 SO4]	**298–328**	**(−0.951)–(−1.021)**	**23.75**	**0.2345**	[132]
[BMIM] [MDEGSO4]	298–308	(−1.064)–(−1.087)	0.31	0.0033	[133]
[C12 3 M IM] [BF4]	308–318	(0.245)–(0.142)	198	0.3664	[120]
[EMIM] [MeSO3]	**312–332**	**(−1.390)–(−1.331)**	**3.19**	**0.0439**	[134]
[C10C10 MIM] [NTF2]	323–343	(−0.037)–(−0.281)	61	0.0495	[134]
[N6111][NTF2]	322–352	(0.149)–(−0.044)	70.42	0.0233	[135]
[EMIM] [N(CN) 2]	**322–343**	**(−0.820)–(−0.891)**	**15**	**0.1295**	[135]
[1B1M Pyrro] [NTF2]	323–343	(0.336)–(0.165)	66.28	0.1581	[136]
[1M1C3 Pyrro] [NTF2]	323–343	(0.322)–(0.139)	37.75	0.0887	[136]
[EMIM] [CF3SO3]	**313–333**	**(−0.328)–(−0.385)**	**11.4**	**0.0418**	[137]
[COC2MIM] [NTF2]	332–353	(0.048)–(−0.174)	683	0.3678	[14]
[CyC3 MIM][N (CN)2]	312–332	(−0.527)–(−0.544)	10.5	0.0561	[14]
[(OC1)2IM] [NTF2]	312–323	(0.095)–(0.058)	32.6	0.0278	[14]
[Hyd EMIM] [NTF2]	322–342	(−0.116)–(−0.223)	37.76	0.0594	[14]
[OMIM][NTF2]	323–343	(0.076)–(−0.083)	150	0.1215	[99]

[a]bold means validation set.

[19–21], which features several methods of internal and external validations in its environment.

This work shows the advantages of QSPR/QSAR approach-based COSMO-RS descriptors in comparison with GCM by Thangarajoo et al. [5], which was based on the functional group descriptors. In this study, a much larger dataset (i.e., 780 total datapoints) including more structural variations of cation and anion has been used in comparison with studied dataset (i.e., 158 total datapoints) by Thangarajoo et al. [5]. The

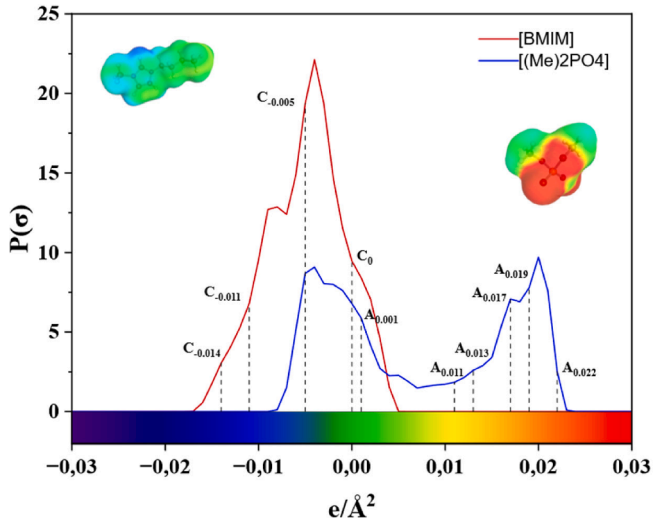

Fig. 2. Demonstration of some cationic and anionic descriptors (i.e., values of probability (amount) at some specific charge densities (SCD)) for [BMIM] cation and [(Me)2PO4] anion.

developed predictive and reliable QSPR/QSAR model aids the chemical engineering community to select the proper ILs for the specific applications.

2. Method

2.1. Basic theory

In this study, the effect of temperature on the IDAC of MeOH in ILs was included as an independent variable based on the van't Hoff equation. Van't Hoff equation expresses the relationship between IDAC of MeOH in ILs and temperature as below (Eq. (3)):

$$ln\left(\gamma_{MeOH}^{\infty}\right) = \frac{D}{T} + E \tag{3}$$

where 'D' and 'E' are adjustable parameters which depend on the molecular descriptors and their weights determined by the QSPR method. In this study, the most important COSMO-RS descriptors (points of specific charge densities) are applied to distinguish the effect of cation and anion structural variations as well as the effect of temperature. As mentioned earlier, the effect of temperature on IDAC of MeOH in the ILs varies with the nature of the ILs. The ln (γ_{MeOH}^{∞}) can be split into its respective entropic and enthalpic components [5]. The partial molar excess enthalpy (*i.e.*, $\Delta H_{IL}^{E,\infty}$) and entropy (*i.e.*, $\Delta S_{IL}^{E,\infty}$) of each IL at infinite dilution can be calculated using 'D' and 'E' in Eq. (3), respectively. For a majority of ILs, the IDAC value of MeOH decreases as temperature increases, however for a limited amount of ILs the opposite behavior has been observed. Therefore, the predictive QSPR/QSAR based-COSMO-RS model should be considered this point well. Hence, the sign of 'D' parameter should be varied with respect of nature of ILs. It means that the sign of 'D' parameter is often '+' that stating the values of IDAC of MeOH in the majority of ILs decrease. Otherwise, the sign of 'D' parameter is rarely '-' that stating the values of IDAC of MeOH in other ILs increase. In brief, the included ILs in this study belong to three different groups with increasing temperature: 1) the values of IDAC of MeOH decrease, 2) the values of IDAC of MeOH increase 3) the values of IDAC of MeOH are almost constant (see Fig. 1).

As can be seen in Fig. 1, there are qualitatively three different IDAC temperature behavior patterns. MeOH in [HMIM][NTF_2], [EMIM][$B(CN)_4$], and [1B1MPyrro][FSI] belongs to the first group of ILs, where IDAC values decrease with increasing temperature. MeOH in [N8888][NTF_2] and [P1444][TOS] belong to the second group, where IDAC values increase with increasing temperature. MeOH in [1B1MPyrro][SCN] and [EMPy][$EtSO_4$] is an example of the third group, where IDAC is nearly temperature invariant.

2.2. Dataset

According to the collected experimental data [6,8,9,10,11,14,22–137], an extensive dataset has been created for QSPR/QSAR studies. The detail of this dataset can be found in Table 1 and Tables S1 and S2. All in all, 780 datapoints including 131 unique ILs (57 cations and 25 anions) at wide range of temperature (around 300–400 K) with above-described features are listed in Table 1.

2.3. QSPR method

Thangarajoo et al. [5], have mentioned that 'QSPR' method is not as efficient as GCM. For this regard, further investigations are still required to probe this issue. Also, different aspects of QSPR method such as variable (or descriptor) selection, internal and external validations, and model assessment using statistical parameters should be done in the related software called 'QSARINS' [19–21]. This study will try to show the advantages of QSPR method using new kind of descriptors.

Table 2
Applied statistical parameters in this study.

Introduced parameters	Introduced parameters equations	Eqs. No
Coefficient of determination	$R^2 = 1 - \frac{\sum_{i=1}^{n}\left(Y_i^{exp} - Y_i^{pre}\right)^2}{\sum_{i=1}^{n}\left(Y_i^{exp} - \overline{Y}_i\right)^2}$	(4)
Adjustable coefficient of determination	$R^2_{Adj} = 1 - (1\text{-}R^2) \times \left(\frac{n-1}{n-p-1}\right)$	(5)
Leave-one-out cross-validated coefficient of determination	$Q^2_{LOO\text{-}CV} = 1 - \frac{\sum_{i=1}^{n}\left(Y_i^{exp} - Y_i^{pre-CV}\right)^2}{\sum_{i=1}^{n}\left(Y_i^{exp} - \overline{Y}_i\right)^2}$	(6)
Fisher function	$F = \frac{\sum_{i=1}^{n}\left(Y_i^{pre} - \overline{Y}_i\right)^2/p}{\sum_{i=1}^{n}\left(Y_i^{exp} - Y_i^{pre}\right)^2/n-p-1}$	(7)
Standard residual	$S = \sqrt{\frac{\sum_{i=1}^{n}\left(Y_i^{exp} - Y_i^{pre}\right)^2}{n-p-1}}$	(8)
root mean square error (RMSE)	$RMSE = \sqrt{\frac{\sum_{i=1}^{n}\left(Y_i^{exp} - Y_i^{pre}\right)^2}{n}}$	(9)
Average absolute deviation	$AAD = \frac{\sum_{i=1}^{n}\left(\lvert Y_i^{exp} - Y_i^{pre}\rvert\right)}{n}$	(10)
Average Absolute relative deviation %	$AARD\% = \frac{\sum_{i=1}^{n}\left(\lvert Y_i^{exp} - Y_i^{pre}\rvert\right)/Y_i^{exp}}{n} \times 100$	(11)
maximum Leverage	$h^* = 3(p+1)/n$	(12)

Y_i^{exp}, Y_i^{pre}, $\overline{Y}_i$, n, and p demonstrate experimental values (ln-Based), predicted values (ln-Based), average experimental values (ln-Based), the number of the experimental dataset, and the number of employed descriptors, respectively.

2.3.1. Calculation of COSMO-based molecular descriptors

Molecular descriptors are from σ-profile which is calculated via COSMO-RS theory [138–141]. Sigma profiles are taken from database (COSMObase 2023) which is provided in COSMOtherm 2023 software [142], and the chosen sigma profiles were calculated by using TZVP-basis set. Descriptor values are taken from lowest energy configuration of cation and anion molecules.

In a nutshell, sigma profile is 2D representation of 3D surface polarities of molecules shown in Fig. 2. The x-axis and y-axis are related to the strength of surface charge density (SCD) and the probability (amount) of finding this surface charge density, respectively. Sigma profile is calculated with 0.001 interval and typically varies from −0.03 to 0.03 e/Å^2. In this study, descriptors have been selected from sigma profile, like the amount of specific surface charge density demonstrated in Fig. 2.

2.3.2. Model development

Since both cation and anion structures are changing in dataset, 'D' and 'E' in Eq. (3) must distinguish the effect of cation and anion structures on ln (γ^{∞}_{MeOH}). For model construction, the suitable descriptors must be selected from 61 descriptors (61 points from −0.03 to + 0.03 with 0.001 step). There are well-known methods of variables selection such as genetic algorithm (GA) method [143], artificial neural network (ANN) [144], replacement method (RM) [145]. In this study, GA was used to build MLR QSPR models-based COSMO descriptors. The details of the GA-MLR algorithm can be found elsewhere [146,147]. It should be mentioned that the QSARINS software was applied to develop the GA-MLR models.

2.3.3. Statistical parameters

The goodness-of-fit of QSPR model should be carefully checked using the standard statistical parameters, including coefficient of determination (R^2), leave-one-out cross-validated coefficient of determination ($Q^2_{LOO\text{-}CV}$), adjustable coefficient of determination (R^2_{Adj}), average absolute relative deviation (%AARD), average absolute deviations (AAD), Fisher function (F), root mean square error (RMSE), standard residual (S), and maximum (or critical) leverage (h*). More detailed information regarding the statistical parameters used in this study can be found in

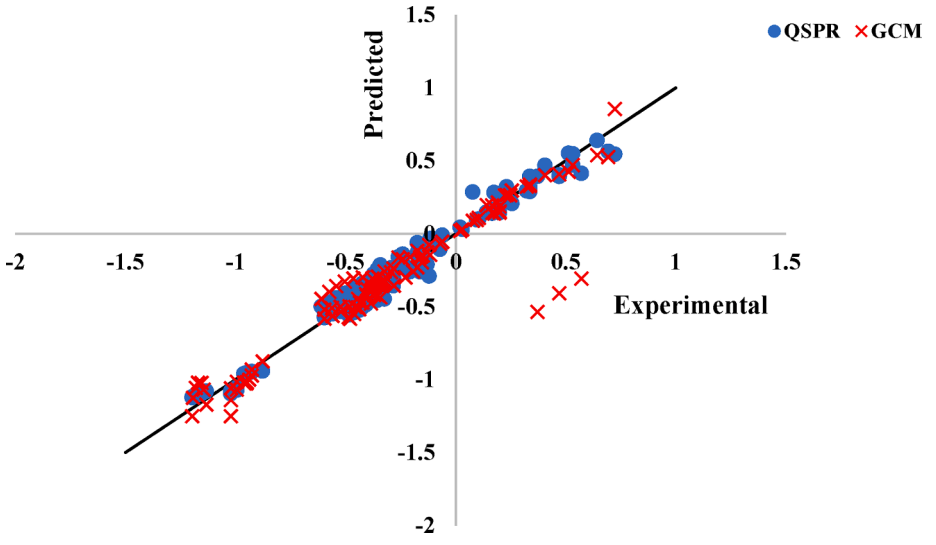

Fig. 3. A comparison between QSPR and GC approaches in the prediction of ln (IDAC) of MeOH in ILs at different temperatures (119 datapoints).

Table 3
Developed QSAR/QSPR models for the overall and training statuses.

Status	Number of datapoints	Model	Eq. No
Overall	780	$\ln\left(\gamma^{\infty}_{MeOH}\right) = \frac{(-1744.7030C-0.020)+(-1.8554C0)+(-1707.6825A-0.012)+(872.1541A-0.010)+(-26.4274A0.013)+(-29.3335A0.017)+(-36.7695A0.019)+(-173.2812A0.022)+789.7839}{T} + (0.0582C\text{-}0.014)+(0.0606C\text{-}0.011)+(0.0355C\text{-}0.005)+(-0.0093\ A0.001)+(0.0054\ A0.011)\text{-}3.0092$	(16)
Training[a]	615	$\ln\left(\gamma^{\infty}_{MeOH}\right) = \frac{(-1816.5636C-0.020)+(-2.1398C0)+(-1123.4926A-0.012)+(600.1665A-0.010)+(-26.0767A0.013)+(-27.2105A0.017)+(-35.3253A0.019)+(-172.8690A0.022)+805.9100}{T} + (0.0672C\text{-}0.014)+(0.0582C\text{-}0.011)+(0.0374C\text{-}0.005)+(-0.0048\ A0.001)+(0.0105\ A0.011)\text{-}3.1615$	(17)

[a] 165 datapoints were set aside into validation set.

Table 2 (Eqs. (4)–(12)).

Applicability of Domain (AD) analysis as a vital concept of QSPR approach should be considered. It allows [148]: 1) the uncertainty in prediction, and 2) the extent of extrapolation of QSPR models [149,150]. For prediction of IDAC values of MeOH in new ILs, it is essential that new ILs lie within the same AD space. It means that the new ILs should be physicochemically, biologically, or structurally similar with molecules used for model development (i.e., training set). The more space of AD, the more reliable predictions of new ILs. To carry out the external validation using validation set, it is essential to ensure that the validations set of molecules is inside of QSPR model's AD [151].

The space of AD can be specified using two main parameters: 1) the leverage values (h_i) 2) the standardized residual (SDR). SDR is defined as Eq. (13):

$$SDR = \frac{Y_i^{exp} - Y_i^{pre}}{\sqrt{\frac{\sum_{m=1}^{n}\left(Y_i^{exp} - Y_i^{pre}\right)^2}{n}}} \tag{13}$$

h_i, represents a measure of a molecule's distance from the center of the training set. It is needed to determine whether new ILs are within the applicability of domain of the developed QSPR model or not. The parameter can be calculated with Eq. (14).

$$h_i(\text{or Leverage}(i)) = z_i \cdot \left(Z_i^T Z_i\right)^{-1} \cdot z_i^T \tag{14}$$

where z_i and Z are the descriptor row vector of point i, and a n × p matrix of descriptors for compounds derived from the training set, respectively. AD of developed QSPR models can be obtained in QSARINS software for each model and the maximum leverage (i.e., h*) can be calculated using Eq. (12).

2.3.4. Internal and external validations

After building of QSAR/QSPR model, it is essential to conduct internal and external validations on the training (approx. 80 % of main dataset) and validation (approx. 20 % of main dataset) sets, respectively. Regarding the internal validation, Y-Scrambling, leave multi out −cross validation (LMO-CV), and leave one out −cross validation (LOO-CV) methods should be conducted on the developed QSAR/QSPR model. In fact, these methods were performed on the training set (not validation set). Regarding the external validation, the prediction capability of developed QSAR/QSPR model is evaluated using a validation set. Both internal and external validations of QSPR models can be carried out in QSARINS software one by one.

3. Results and discussion

3.1. A comparison with former model based-GCM

Unlike the cation structures which were decomposed into many functional groups, Thangarajoo et al. [5] surprisingly did not decompose anion structures in a similar manner. For this regard, 'How does GCM distinguish the effect of other anions such as Cl, Br, etc.' Second, the frequencies of the second and third groups of ILs in the former studied dataset by Thangarajoo et al. [5] were not good enough. As already observed in Fig. 1, there were other ILs from second and third groups which were not considered by Thangarajoo et al. [5]. Therefore, it seems that it is better to use an extensive dataset with more abundant variations of cation and anion. In this study, the first step is to verify the accuracy of QSAR/QSPR approach-based COSMO-RS descriptors. In the following, a QSAR/QSPR based on the van't Hoff equation (i.e., Eq. (3)) has been developed for 119 datapoints of formerly studied dataset for which all the needed COSMO-RS descriptors were available in our database. The advantage of such a model is that the model can predict the IDAC of MeOH in those ILs including other anions such as Cl and Br which were not included in the dataset. The details of 119 datapoints for

Table 4
The values of statistical parameters of selected QSPR models for both training and validation sets.

Eqs. No	Sets	Number of datapoints	R2	R2-Adj	Q2-LOO	Q2-LMO	F	S	RMSE	AARD%	AAD
(16)	Overall status	780	0.92	0.91	0.91	0.91	587	0.2471	0.2447	73	0.1864
(17)	Training	615	0.92	0.92	0.92	0.92	514	0.2423	0.2393	77	0.1829
	Validation	165	0.85	–	–	–	–	–	0.2926	53	0.2034

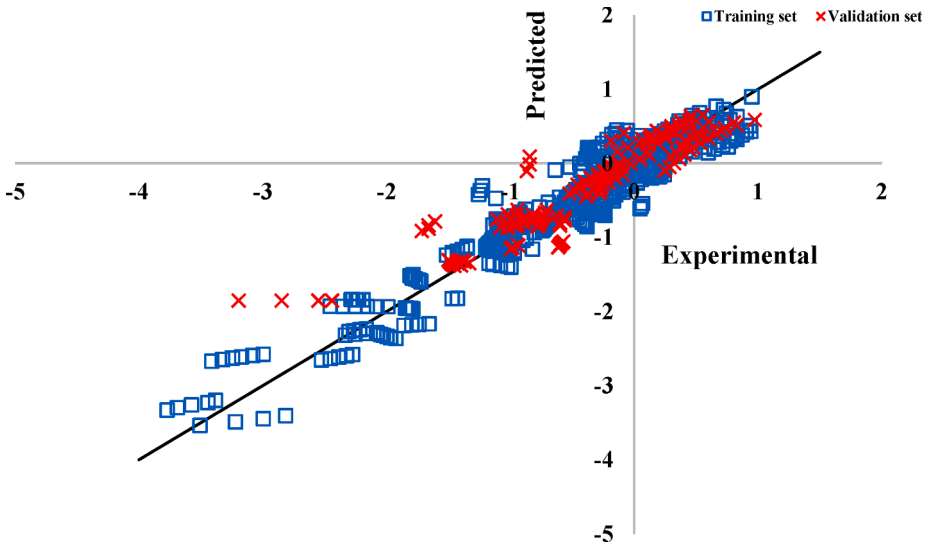

Fig. 4. The predicted versus experimental values (ln-based) for both of training and validation sets using Eq. (17).

development of this QSPR model can be found in the Supporting Information (Table S3). This model (i.e., Eq. (15)) has been built using all datapoints in overall status (without dividing into training and validation sets).

$$\ln(\gamma^{\infty}_{MeOH}) = \frac{(-298.5512C - 0.016) + (1144.3569A - 0.005) + (29.4340A0.019) + 132.1289}{T} + (0.2076\,\mathrm{C} - 0.015) + (0.0598\,\mathrm{C} - 0.013) + (0.0483\,\mathrm{C} - 0.009) + (-3.5353\,\mathrm{A} - 0.005) + (0.0734\,\mathrm{A}0.011) + (-0.1834\,\mathrm{A}0.013) + (0.0747\,\mathrm{A}0.014) + (-14.4842\,\mathrm{A}0.021) - 0.9588 \quad (15)$$

Four points of specific charge density from sigma profile (i.e., 'C-0.016′, 'C-0.015′, 'C-0.013′, and 'C-0.009′) are the cationic descriptors, and six points of specific charge density (i.e., 'A-0.005′, 'A0.011′, 'A0.013′, 'A0.014′, 'A0.019′, and 'A0.021′) are the anionic descriptors. The values of probability (amount) at above points of specific charge density for each cation and anion are used and important for the prediction of IDAC of MeOH in ILs.

As can be seen in Fig. 3, QSPR method can be as efficient as GCM. The R^2 and AARD% values for QSPR model (i.e., Eq. (15)) and GCM were (0.98 and 19.5 %) and (0.90 and 17 %), respectively. After performing this simple comparison, it was found that QSAR/QSPR approach using COSMO-RS descriptors can be used as a robust and reliable tool for prediction of IDAC of MeOH in large space of ILs at a wide range of temperature which was already described in the dataset section.

3.2. Developed QSAR/QSPR models

In this study, an extensive dataset including 57 cations, 25 anions, and 780 datapoints was divided to training and validation sets for performing of internal and external validations. Some ILs were set intentionally aside in the validation set to guarantee presence of ILs with new structures for both cation and anion. Among the specified ILs as the validation set (see Table 1, **Bold** ILs), the structures for both cation and anion in [EMIM][$B(CN)_4$], [C_{10}MIM][$B(CN)_4$], [EMIM][FSI], [N2228][FSI], [1M1C_3Pip][FSI], [1M1C_3Pyrro][FSI], [EMIM][C_8SO_4], [1,3 MMIM][$MeSO_4$], and [EMIM][H_2SO_4] were absence in the training set.

In this study, leave-one-ion-out cross-validation [152,153] has been applied for assisting in developing robust QSPR models of ILs. The main aim of this categorization is to investigate the QSAR/QSPR's prediction capability for new structures of cation and anion.

The QSAR/QSPR models which were developed in overall status (Eq. (16)) as well as training status (Eq. (17)) are indicated in Table 3.

The values of statistical parameters of each selected model are shown in Table 4.

As indicated in Table 4, the obtained values of Q^2_{LOO} (as internal validation) of each status (either overall or training status) were high which are confirming that each model has acceptable capability for prediction of IDAC of MeOH in studied ILs in a wide range of temperatures (see Table 1). Also, LMO-CV and Y-scrambling techniques have been done on the training set in the QSARINS software for each selected QSPR model and results confirmed the validity of each model. As external validation, it is also shown that IDAC of MeOH in ILs of validation set predicted with enough accuracy based on the obtained values of AAD and RMSE. The calculated values of AARD% for some ILs are relatively high in Table 1, which are apparently affecting the reported average values for training and validation sets in Table 4 (i.e., 77 and 53, respectively). When the number of datapoints with experimental values so close to zero (i.e., between −0.1 to + 0.1) increases in a dataset (like

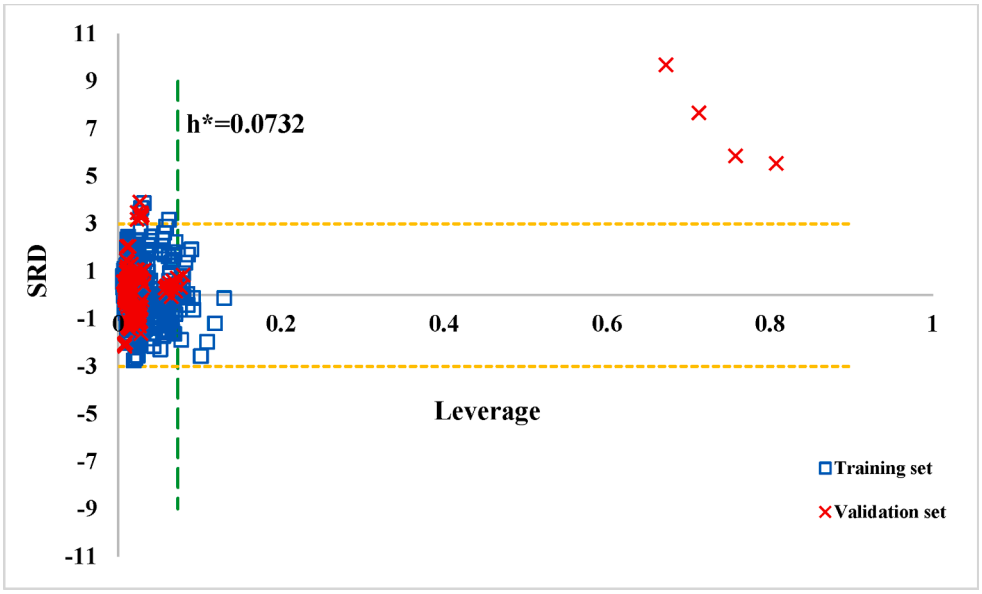

Fig. 5. Williams plot for training and validation sets using Eq. (17).

Table 5
The value of 'D' parameter of van't Hoff equation with its sign in comparison with Exp-slope for three different groups of ILs.

Group of ILs	Sets	Studied ILs in Table 1	Value of 'D' parameter in van't Hoff equation or Cal-slope (Eq. (17))	Exp-slope (ln IDAC-Exp vs 1/T)
First	Training	[Et3S][NTF2]	+663	+863
	validation	[C10MIM][B(CN)4]	+535	+662
Second	Training	[Hyd EM Pyrro][MMPO4]	−216	−769
	Training	[P66614][Cl]	−277	−1236
	validation	Not found[a]	–	–
Third	Training	[1,3 BB IM][Br]	–32	−151
	validation	[EMIM][MDEGSO4]	+230	+264

[a] there were no ILs from the second group in the validation set.

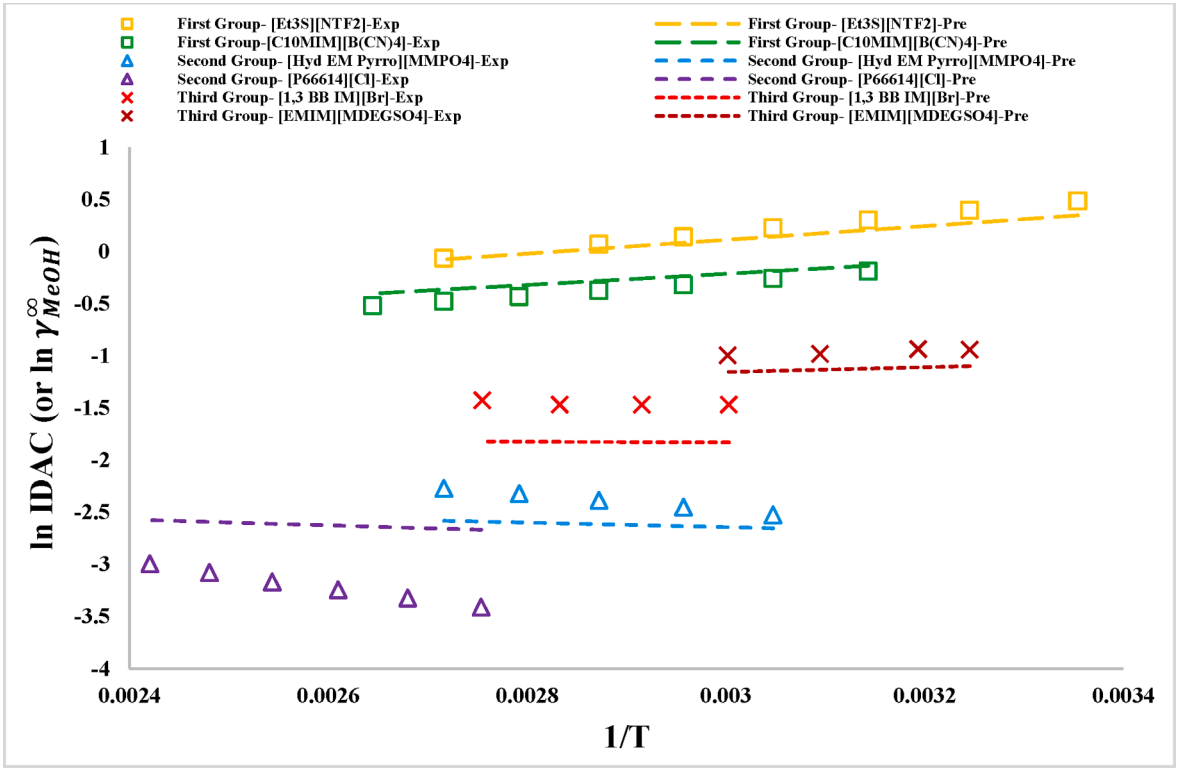

Fig. 6. The capability of QSAR/QSPR model in the prediction of idac of meoh in three different groups of ils (seeTable 5).

Table 6
Calculated partial molar excess enthalpy (*i.e.*, $\Delta H_{IL}^{E,\infty}$) and entropy (*i.e.*, $\Delta S_{IL}^{E,\infty}$) of each IL at infinite dilution using molecular descriptors in 'D' and 'E' parameters of van't Hoff equation.

IL	$\Delta H_{IL}^{E,\infty}$ (J·(mol)$^{-1}$)	$\Delta S_{IL}^{E,\infty}$ (J·(K·mol)$^{-1}$)	IL	$\Delta H_{IL}^{E,\infty}$ (J·(mol)$^{-1}$)	$\Delta S_{IL}^{E,\infty}$ (J·(K·mol)$^{-1}$)
[HMIM][NTF2]	5424.09	15.08	[C6-isoquinolinium][SCN]	2605.68	16.27
[HMIM][NTF2]	5424.09	15.08	[N-C3OH MIM][SCN]	2916.19	12.87
[1B4MPy][SCN]	2800.41	15.33	[C6Py][Br]	−236.73	15.61
[1B1MPyrro][SCN]	2850.35	15.80	[1B3M Py][CF3SO3]	3818.42	15.35
[BMIM][SCN]	2828.45	14.65	[COC2 MPyrro][FAP]	6599.12	15.53
[EMIM] [SCN]	2879.72	14.89	[HydEMIM][FAP]	5592.88	15.82
[BMIM][CF3SO3]	3840.18	15.16	[Hyd EM Pyrro][MMPO4]	−1799.82	16.58
[Et3S][NTF2]	5513.91	15.61	[BMIM][NTF2]	5530.09	14.76
[1B4MPy][NFT2]	5502.05	15.44	**[EMIM] [NO3]**	2043.28	15.20
[P1444][TOS]	1298.34	16.82	[BMIM][MeSO3]	1377.07	15.25
[HMIM][SCN]	2722.46	14.97	**[EMIM] [EtSO4]**	2932.99	15.52
[1B1MPyrro][CF3SO3]	3862.07	16.32	[P66614][Bis (M)3 C5 Phos]	−3932.33	16.85
[P66614][BF4]	3025.16	13.47	**[EMIM] [FAP]**	6581.54	16.10
[P66614][PF6]	5392.20	15.38	**[EMIM] [B(CN)4]**	4852.11	15.06
[C10MIM] [B(CN)4]	4453.18	15.13	[HMIM][BOB]	5477.30	14.15
[EMIM] [B(CN)4]	4852.11	15.06	[BMIM][BOB]	5583.29	13.83
[OMIM][NO3]	1766.06	15.15	[1M3C3 IM][Br]	−125.90	14.93
[BMIM][NO3]	1992.01	14.95	[BMIM][BF4]	4164.96	12.92
[HydEMIM][BF4]	3227.58	12.87	**[EMIM] [MDEGSO4]**	1913.60	15.35
[N-C3OHPy][NTF2]	5603.10	13.87	**[EMIM] [C8 SO4]**	3017.08	16.01
[BMIM][CLO4]	2841.17	13.89	[OMIM][PF6]	6306.05	15.02
[OMIM][MDEGSO4]	1636.38	15.31	[BMIM][PF6]	6532.00	14.82
[N2228] [FSI]	6028.11	15.61	**[BMIM] [MeSO4]**	2953.31	15.13
[1B1MPyrro] [FSI]	6335.37	15.29	**[EMIM] [H2SO4]**	−43.26	15.26
[EMIM] [MESO3]	1428.34	15.49	[1B4M Py][BF4]	4136.93	13.60
[1B1MPyrro][C(CN)3]	4258.23	15.89	**[EMIM] [NTF2]**	5581.36	15.00
[1M1C3Piper][NTF2]	5562.84	14.81	[E MM IM][NTF2]	5574.65	15.72
[C12MIM][NTF2]	5061.35	15.10	[N4111][NTF2]	5595.84	15.46
[1B1MPyrro] [B(CN)4]	4822.74	15.97	[P14666][N(CN)2]	1872.23	15.60
[HMIM] [B(CN)4]	4694.85	15.14	[P66614][Bis (M)3 C5 Phos]	−3932.33	16.85
[1B1MPyrro][FAP]	6552.17	17.02	[Epy][NTF2]	5594.33	15.14
[N1112OH][NTF2]	4159.77	15.54	**[1,3 MMIM] [MeSO4]**	3072.70	16.19
[1E1MPyrro][Lac]	149.84	16.47	[HMIM][NTF2]	5424.09	15.08
[BMIM][N(CN)2]	3012.04	15.04	[OMIM][NTF2]	5304.13	14.96
[N-C3OHPy][N(CN)2]	3085.05	14.15	[N-C3OH MMor][C(CN)3]	4336.17	14.00
[EMMor][N(CN)2]	3117.28	15.57	**[EMIM] [NTF2]**	5581.36	15.00
[P4444][NTF2]	5290.50	14.22	[P66614][NTF2]	4390.28	15.32
[EMPy][EtSO4]	2905.81	15.92	[BMIM][Cl]	−1165.79	15.28
[BMIM][CF3SO3]	3840.18	15.16	[BMIM][(Me)2PO4]	−1564.58	15.35
[EMIM] [EtSO4]	2932.99	15.52	[3 M 1C14 IM][BF4]	3576.26	13.24
[EMIM] [C(CN)3]	4287.60	14.97	[C12 3 M IM][BF4]	3696.22	13.26
[N-C3OHMIM][N(CN)2]	3099.78	13.26	[3 M 1C14 IM][BF4]	3576.26	13.24
[N-C3OHMMor][N(CN)2]	3111.88	14.31	[CyC3 MIM][N(CN)2]	3105.20	14.53
[1B4MPy][C(CN)3]	4208.29	15.42	[BMIM][BF4]	4164.96	12.92
[BMIM][C(CN)3]	4236.33	14.73	[BMIM][Cl]	−1165.79	15.28
[COC2MPyrro][NTF2]	5598.93	14.42	[1,3 BB IM][Br]	−268.84	14.41
[COC2MMor][NTF2]	5630.48	14.09	[BMIM][PF6]	6532.00	14.82
[COC2MPip][NTF2]	5573.12	13.94	[P66614][NTF2]	4390.28	15.32
[COC2MPip][FAP]	6573.30	15.05	[1E 2,3MM IM][NTF2]	5574.65	15.72
[HydEMIM][FAP]	5592.88	15.82	[1B4M Py][BF4]	4136.93	13.60
[COC2MPyrro][FAP]	6599.12	15.53	[N101011][ClO4]	2127.57	14.71
[COC2 N112][FAP]	6553.27	16.39	[N101011][BF4]	3451.36	13.73
[HMIM][NTF2]	5424.09	15.08	[N1118][NTF2]	5375.27	15.74
[CNMe(M)2iPAm][NTF2]	5625.60	13.59	[N8888][NTF2]	4430.98	14.52
[BzMIM][NTF2]	5566.43	14.23	[N4441][NTF2]	5401.91	14.65
[COC2 Py][NTF2]	5592.40	13.82	[P66614][NTF2]	4390.28	15.32
[OMIM][PF6]	6306.05	15.02	[OMIM][BF4]	3939.01	13.12
[1B1MPip][NTF2]	5527.84	15.24	**[EMIM] [BF4]**	4216.23	13.16
[1H1MPip][NTF2]	5429.82	15.50	[HMIM[]BF4]	4058.97	13.24
[1M1C5Pip][NTF2]	5485.41	15.45	[P66614][FAP]	5390.46	16.42
[1B1MPyrro][FSI]	6335.37	15.29	[HMIM][PF6]	6426.01	15.15
[1M1C3Pyrro] [FSI]	6370.34	14.93	**[BMIM] [C8 SO4]**	2965.81	15.77
[EMIM] [FSI]	6364.74	14.38	[BMIM][MDEGSO4]	1862.33	15.11
[1M1C3Pip] [FSI]	6346.22	14.19	[C12 3 M IM][BF4]	3696.22	13.26
[P66614][Cl]	−2305.60	15.84	**[EMIM] [MeSO3]**	1428.34	15.49
[COC2MMor][FAP]	6630.66	15.19	[C10C10 MIM][NTF2]	4720.13	15.38
[EMIM] [FAP]	6581.54	16.10	[N6111][NTF2]	5496.14	15.81
[N-C3OH MMor][NTF2]	5629.93	14.03	**[EMIM] [N(CN)2]**	3063.31	15.28
[C10C10 MIM][N(CN)2]	2202.08	15.67	[1B1M Pyrro][NTF2]	5551.98	15.91
[Epy][NTF2]	5594.33	15.14	[1M1C3 Pyrro][NTF2]	5586.96	15.55
[C5Py][NTF2]	5506.76	14.97	**[EMIM] [CF3SO3]**	3891.45	15.40
[BPy][NTF2]	5548.69	14.83	[COC2MIM][NTF2]	5580.84	13.66
[HMIM][Cl]	−1271.78	15.60	[CyC3 MIM][N(CN)2]	3105.20	14.53

(*continued on next page*)

Table 6 (*continued*)

IL	$\Delta H_{IL}^{E,\infty}$ (J·(mol)$^{-1}$)	$\Delta S_{IL}^{E,\infty}$ (J·(K·mol)$^{-1}$)	IL	$\Delta H_{IL}^{E,\infty}$ (J·(mol)$^{-1}$)	$\Delta S_{IL}^{E,\infty}$ (J·(K·mol)$^{-1}$)
[HydEMIM][PF6]	5594.62	14.78	[(OC1)2IM][NTF2]	5648.16	16.91
[C10 MIM] [NTF2]	5182.43	15.07	[Hyd EMIM][NTF2]	4592.70	14.71
[Quin6][NTF2]	5426.46	15.06	[OMIM][NTF2]	5304.13	14.96
[Quin8][NTF2]	5306.27	15.11			
[1B1MPyrro][N(CN)2]	3033.94	16.20			
[1B1MPyrro][BOB]	5605.19	14.98			
[1B1MPyrro][B(CN)4]	4822.74	15.97			
[EMIM] [MeSO3]	1428.34	15.49			
[EMIM] [B(CN)4]	4852.11	15.06			
[EMIM] [NTF2]	5581.36	15.00			
[1B1MPip][SCN]	2826.21	15.13			
[C8-isoquinolinium][NTF2]	5185.91	16.35			
[1B1MPyrro][N(CN)2]	3033.94	16.20			

Table 7
The values of ln IDAC-Pseudo Exp of MeOH in some of unique none-studied ILs using Eq. (17).

None-studied ILs	***Temperature (T (K))***							
	298	308	318	328	338	348	358	368
[NTF2]-based ILs								
[P1444][NTF2]	0.2456	0.1751	0.109	0.0469	−0.0115	−0.0666	−0.1185	−0.1677
[N2228][NTF2]	0.1642	0.0955	0.0311	−0.0294	−0.0863	−0.1399	−0.1906	−0.2385
[1E1MPyrro][NTF2]	0.3394	0.266	0.1972	0.1326	0.0718	0.0145	−0.0395	−0.0907
[EMMor][NTF2]	0.4359	0.362	0.2928	0.2278	0.1667	0.1091	0.0546	0.0032
[EMPy][NTF2]	0.3896	0.3168	0.2486	0.1846	0.1243	0.0675	0.0139	−0.0368
[N-C3OHMIM][NTF2]	0.706	0.6324	0.5634	0.4986	0.4376	0.3802	0.326	0.2747
[COC2 N112][NTF2]	0.4021	0.3294	0.2612	0.1971	0.1369	0.0801	0.0265	−0.0242
[C6Py][NTF2]	0.3845	0.3131	0.2462	0.1833	0.1242	0.0685	0.0159	−0.0339
SCN- based ILs								
[C10MIM][SCN]	−0.7986	−0.8311	−0.8616	−0.8902	−0.9171	−0.9425	−0.9664	−0.9891
[OMIM][SCN]	−0.7356	−0.7697	−0.8016	−0.8317	−0.8599	−0.8865	−0.9116	−0.9354
[EMPy][SCN]	−0.6875	−0.7249	−0.7599	−0.7928	−0.8238	−0.853	−0.8805	−0.9065
[1M1C5Pip][SCN]	−0.7212	−0.7577	−0.7919	−0.824	−0.8542	−0.8827	−0.9095	−0.935
[Epy][SCN]	−0.64	−0.6779	−0.7134	−0.7468	−0.7782	−0.8077	−0.8357	−0.8621
[BF4]-based ILs								
[C10MIM][BF4]	−0.0507	−0.1008	−0.1476	−0.1916	−0.2331	−0.2721	−0.309	−0.3438
[EMPy][BF4]	0.0603	0.0054	−0.046	−0.0943	−0.1398	−0.1826	−0.223	−0.2613

our dataset and unlike former studied dataset by Thangarajoo et al. [5]), it is expectable that the value of AARD% tends to approach to higher value. According to our dataset (see Table 1), it is evident that most ILs have at least one or two ln (IDAC-Exp) values which are so close to zero (i.e., between −0.1 to + 0.1). In other words, there are many of ln (IDAC-Exp) values in our dataset which have been concentrated in this small range (−0.1 to + 0.1) which is about one twentieth (1/20) of whole studied range (−3.77 to + 0.97). ARD% values are naturally high in this range of Ln (IDAC). It means that a small absolute deviation gives a high ARD%. Therefore, it is expected that the value of AARD% (i.e., average of ARD%) for some of ILs becomes high and or very high. As can be seen in Table 1, there are high values of AARD% for [BMIM][CLO_4], [C_{12} 3MIM][BF_4], [P66614][NTF_2], and [COC_2 MIM][NTF_2] which their experimental ranges were (0.067)–(0.048), (0.058)–(−0.054), (0.079)–(−0.147), and (0.048)–(−0.174), respectively. In contrast, the low values of AARD% are experienced for [1E1MPyrro][Lac], [EMIM][$EtSO_4$], [COC_2MPip][FAP], and [BMIM][$(Me)_2PO_4$] which their experimental ranges were (−2.453)–(−1.987), (−0.621)–(−1.081), (0.746)–(0.398), and (−2.333)–(−2.079), respectively. Such problem can be observed in the literature, too. For example, Gonfa et al. [12] applied the QSAR approach for prediction of IDAC of water in ILs. The range of experimental values was approximately in the range of −4 to 2, which is rather close to our dataset range. They reported the R^2 and RMSE values of 0.97 and 0.35, respectively. Since, the statistical parameters and prediction capability of our model are close to them, most likely the unreported values of AARD% are also quite similar to our reported values in Table 4.The proposed QSAR/QSPR model could take into account the effect of temperature on the IDAC of MeOH in majority of studied ILs (the included ILs in Table 1) well and satisfactorily. However, for some ILs the capability of QSAR/QSPR model was not satisfactory. For example, the temperature dependencies of IDAC of MeOH in some ILs such as [BMIM][$MeSO_3$] and [P14666][$N(CN)_2$] were not correct. Such conflict was observed also by Thangarajoo et al. [5]. For example, the values of IDAC of MeOH in [HydEMIM][FAP] were increasing with increasing temperature, while the developed model using GCM by Thangarajoo et al. [5] predicted the opposite.

The plot of predicted versus experimental values for both of training and validation sets which was obtained using QSAR/QSPR model (i.e., Eq. (17)), is shown in Fig. 4.The Williams plot for the training and validation sets which was obtained using QSAR/QSPR model (i.e., Eq. (17)), is shown in Fig. 5. According to this plot, there is only one studied IL in Table 1 (i.e., [EMIM][H_2SO_4] at four temperatures) which can be considered as an outlier. Because this IL, not only has leverage value higher than critical leverage (i.e., h*=0.0732), but also its SRD is higher than + 3. Although the leverage values of some ILs were a little bit higher than critical leverage (h*), but the developed model could predict the IDAC of MeOH in those ILs well.To gain deeper insights into the significance of the 'D' adjustable parameter in the QSAR/QSPR model (i.e., Eq (17)), previously introduced as a parameter within the van't Hoff equation, its role and implications were further analyzed. At first, the slope value of best linear fitting curve for ln (IDAC-Exp) versus 1/T plot was calculated for some representatives of three groups of ILs, and reported in Table 5. As can be seen in Table 5, not only the signs of 'D' can be '+' and sometimes they can be '-', but also, the values of 'D' have consistency with obtained slopes from experimental data (ln (IDAC-Exp) versus 1/T). It means that suggested QSPR model could fit data with

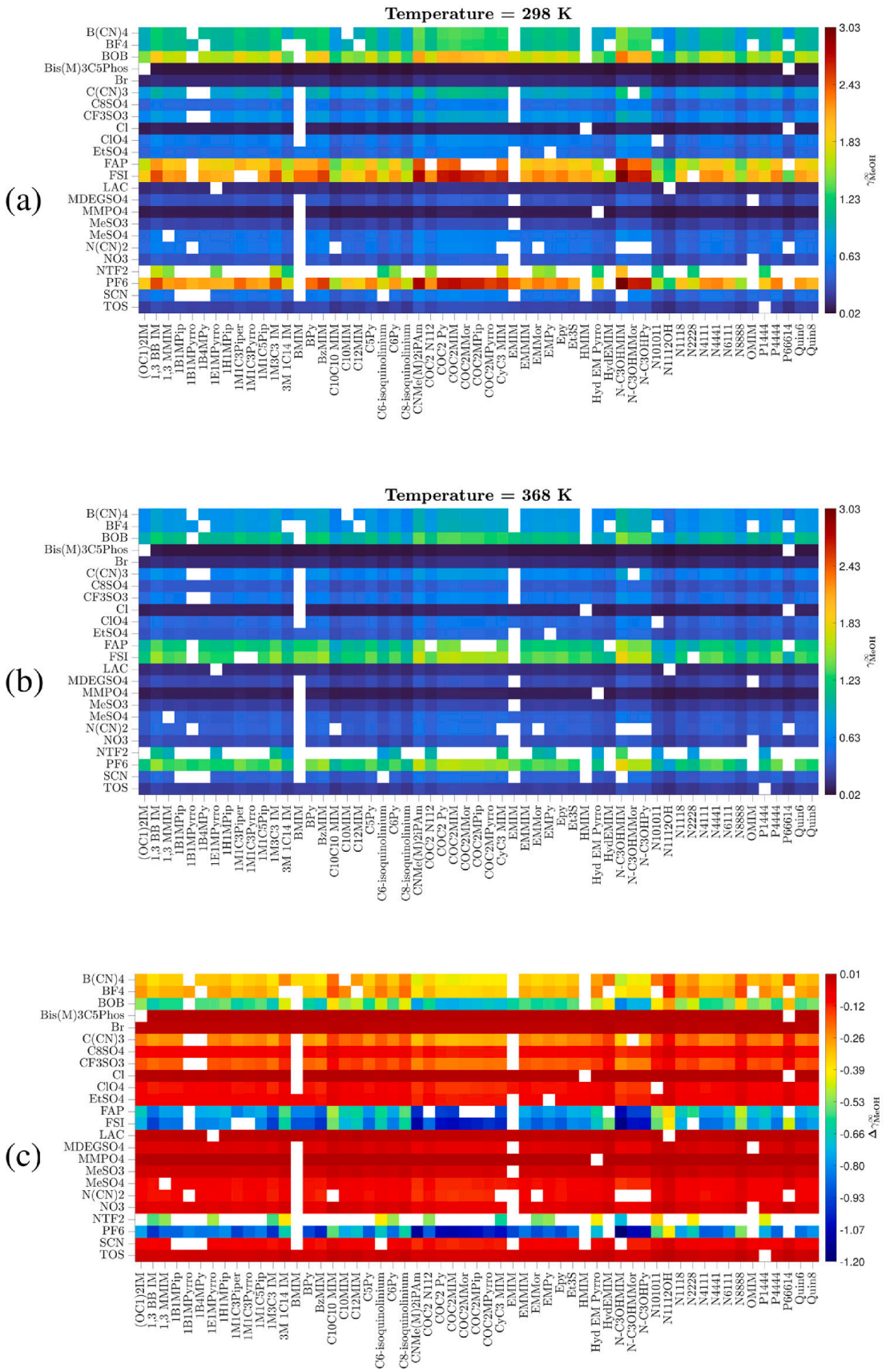

Fig. 7. Predicted IDAC values by QSPR-model at a) 298 K, b) 368 K, and c) difference of IDAC values between temperature 298 and 368 K.

both positive and negative slopes. The accuracy of QSAR/QSPR model for the prediction of IDAC of MeOH in shown ILs in Table 5 at a wide range of temperatures, has been presented in Fig. 6.

As temperature dependency of IDAC of MeOH in ILs can be expressed by physicochemical properties (*i.e.*, $\Delta H_{IL}^{E,\infty}$ and $\Delta S_{IL}^{E,\infty}$), it may be interesting to look at these predicted properties, separately. Although these values are determined indirectly from temperature dependency of IDAC, they may reveal interesting further structure–property relationships. These two properties for each studied IL in Table 1, have been calculated using descriptors in 'D' and 'E' parameters and reported in Table 6. More details can be found in Table S4.Based on the proposed QSAR/QSPR model, a large list including the values of ln IDAC-Pseudo Exp of MeOH in large numbers of none-studied ILs at different temperatures has been provided in the Supporting Information Excel File (Table S5). The values of ln IDAC-Pseudo Exp of MeOH in some of the unique none-studied ILs, where the combination of the anion or cation was frequently present in the training set, have been tabulated in Table 7. The leverage values of these ILs were lower than h*, which means that applying the QSPR model on these ILs is practical.Predicted values of IDAC of MeOH in many new ILs (different combinations of cation and anion), which were not included in our dataset, are shown at Fig. 7. Here, few conclusions can be made: i) the effect of anion is greater than cation, and ii) by increasing temperature, the IDAC values decreased in majority of ILs. Only in few ILs, the IDAC value slightly increases by increasing temperature. [Bis(M)3C5Phos]$^-$ [Cl]$^-$, [Br]$^-$, and [MMPO4]$^-$ anions showed an increasing trend. However, the increase of IDAC value in the presence of these anions is small.

4. Conclusion

The developed QSAR/QSPR model could successfully predict the IDAC value of MeOH in ILs as a function of temperature. The versatility of the model is displayed by the ability to predict the effect of temperature both the increase and decrease of the IDAC of MeOH which is determined by the structure of the IL. The present model succeeds to predict the temperature dependency of IDAC of MeOH for new ILs.The values of statistical parameters (RMSE, AAD, R^2, and $Q^2_{LOO\text{-}CV}$) were acceptable for both training and validation sets. The obtained values of RMSE parameter were 0.23 and 0.29 for training and validation sets, respectively, expressing the high prediction capability of QSPR model for the studied dataset. Based on the internal and external validations and the leverage value of ILs and AD of model, IDAC of MeOH in huge number of ILs, which had not been experimentally studied, can be successfully predicted by presented QSPR model.

5. Nomenclature

See *Supporting Information* File (Table S6).

CRediT authorship contribution statement

Ali Ebrahimpoor Gorji: Writing – review & editing, Writing – original draft, Visualization, Validation, Software, Methodology, Investigation, Formal analysis, Data curation, Conceptualization. **Juho-Pekka Laakso:** Writing – review & editing, Visualization, Methodology, Data curation, Conceptualization. **Ville Alopaeus:** Writing – review & editing, Supervision, Project administration, Funding acquisition, Formal analysis, Conceptualization. **Petri Uusi-Kyyny:** Writing – review & editing, Visualization, Supervision, Project administration, Formal analysis.

Declaration of competing interest

The authors declare that they have no known competing financial interests or personal relationships that could have appeared to influence the work reported in this paper.

Acknowledgement

This work was finically supported by the Academy of Finland 'In-situ equilibrium shifting in CO2 utilization reactions by novel absorbents (CO2Shift)' Project (351113). The authors gratefully and thankfully appreciate to **Prof. Paola Gramatica** (University of Insubria) for providing the free license of QSARINS software for the development of Multilinear Regression models.

Appendix A. Supplementary data

Supplementary data to this article can be found online at https://doi.org/10.1016/j.fuel.2025.134674.

Data availability

Data will be made available on request.

References

[1] Bhongale PV, Amonkar AA, Joshi SS, Mali NA. Kinetic study on alkylation of hydroquinone with methanol over SO3H functionalized Brønsted acidic ionic liquids. *Can J Chem Eng* 2022;100(10):2986–96.
[2] Liu K, Liu C. Synthesis of dimethyl carbonate from methanol and CO 2 under low pressure. *RSC Adv* 2021;11(57):35711–7.
[3] Pawar AA, Lee D, Chung WJ, Kim H. Understanding the synergy between MgO-CeO2 as an effective promoter and ionic liquids for high dimethyl carbonate production from CO2 and methanol. *Chem Eng J* 2020;395:124970.
[4] Maia FM, Tsivintzelis I, Rodriguez O, Macedo EA, Kontogeorgis GM. Equation of state modelling of systems with ionic liquids: Literature review and application with the Cubic Plus Association (CPA) model. *Fluid Phase Equilib* 2012;332:128–43.
[5] Thangarajoo N, Matheswaran P, Johari K, Kurnia KA. Overview of Activity Coefficient of Methanol at Infinite Dilution in Ionic Liquids and their Modeling using Group Contribution Model. *J Chem Eng Data* 2019;64(4):1760–9.
[6] Domańska U, Marciniak A. Activity coefficients at infinite dilution measurements for organic solutes and water in the ionic liquid 4-methyl-N-butyl-pyridinium bis (trifluoromethylsulfonyl)-imide. *J Chem Thermodyn* 2009;41(12):1350–5.
[7] Li Y, Wang LS, Li MY, Tian NN. Activity Coefficients at Infinite Dilution of Organic Solutes in 1-Decyl-3-methylimidazolium Tetrafluoroborate Using Gas–Liquid Chromatography. *J Chem Eng Data* 2011;56(4):1704–8.
[8] Domańska U, Marciniak A, Królikowska M, Arasimowicz M. Activity coefficients at infinite dilution measurements for organic solutes and water in the ionic liquid 1-hexyl-3-methylimidazolium thiocyanate. *J Chem Eng Data* 2010;55(7):2532–6.
[9] Domańska U, Redhi GG, Marciniak A. Activity coefficients at infinite dilution measurements for organic solutes and water in the ionic liquid 1-butyl-1-methylpyrrolidinium trifluoromethanesulfonate using GLC. *Fluid Phase Equilib* 2009;278(1–2):97–102.
[10] Mutelet F, Djebouri H, Baker GA, Ravula S, Jiang B, Tong X, et al. Study of benzyl- or cyclohexyl-functionalized ionic liquids using inverse gas chromatography. *J Mol Liq* 2017;242:550–9.
[11] Mutelet F, Baker GA, Zhao H, Churchill B, Acree Jr WE. Development of Abraham model correlations for short-chain glycol-grafted imidazolium and pyridinium ionic liquids from inverse gas-chromatographic measurements. *J Mol Liq* 2020;317:113983.
[12] Gonfa G, Bustam MA, Shariff AM, Muhammad N, Ullah S. Quantitative structure–activity relationships (QSARs) for estimation of activity coefficient at infinite dilution of water in ionic liquids for natural gas dehydration. *J Taiwan Inst Chem Eng* 2016;66:222–9.
[13] Gonfa G, Bustam MA, Sharif AM, Mohamad N, Ullah S. Tuning ionic liquids for natural gas dehydration using COSMO-RS methodology. *J Nat Gas Sci Eng* 2015;27:1141–8.
[14] Revelli AL, Mutelet F, Jaubert JN, Garcia-Martinez M, Sprunger LM, Acree Jr WE, et al. Study of ether-, alcohol-, or cyano-functionalized ionic liquids using inverse gas chromatography. *J Chem Eng Data* 2010;55(7):2434–43.
[15] Gorji AE, Sobati MA, Alopaeus V, Uusi-Kyyny P. Toward solvent screening in the extractive desulfurization using ionic liquids: QSPR modeling and experimental validations. *Fuel* 2021;302:121159.
[16] Gorji AE, Sobati MA. Toward molecular modeling of thiophene distribution between the ionic liquid and hydrocarbon phases: Effect of hydrocarbon structure. *J Mol Liq* 2019;287:110976.
[17] Gorji AE, Sobati MA. How anion structures can affect the thiophene distribution between imidazolium-based ionic liquid and hydrocarbon phases? A theoretical QSPR study. *Energy Fuel* 2019;33(9):8576–87.
[18] Gorji AE, Sobati MA. Effect of the cation structure on the thiophene distribution between the ionic liquid with NTf2 anion and the hydrocarbon rich phases: A QSPR study. *J Mol Liq* 2020;313:113551.

[19] Gramatica P. Principles of QSAR modeling: comments and suggestions from personal experience. *International Journal of Quantitative Structure-Property Relationships (IJQSPR)* 2020;5(3):61–97.

[20] Gramatica P, Sangion A. A historical excursus on the statistical validation parameters for QSAR models: a clarification concerning metrics and terminology. *J Chem Inf Model* 2016;56(6):1127–31.

[21] Gramatica, P., Chirico, N., Papa, E., Cassani, S., & Kovarich, S. (2013). QSARINS: A new software for the development, analysis, and validation of QSAR MLR models.

[22] Heintz A, Verevkin SP, Lehmann JK, Vasiltsova TV, Ondo D. Activity coefficients at infinite dilution and enthalpies of solution of methanol, 1-butanol, and 1-hexanol in 1-hexyl-3-methyl-imidazolium bis (trifluoromethyl-sulfonyl) imide. *J Chem Thermodyn* 2007;39(2):268–74.

[23] Dobryakov YG, Tuma D, Maurer G. Activity coefficients at infinite dilution of alkanols in the ionic liquids 1-butyl-3-methylimidazolium hexafluorophosphate, 1-butyl-3-methylimidazolium methyl sulfate, and 1-hexyl-3-methylimidazolium bis (trifluoromethylsulfonyl) amide using the dilutor technique. *J Chem Eng Data* 2008;53(9):2154–62.

[24] Domanska U, Królikowska M. Measurements of activity coefficients at infinite dilution in solvent mixtures with thiocyanate-based ionic liquids using GLC technique. *J Phys Chem B* 2010;114(25):8460–6.

[25] Domańska U, Laskowska M. Measurements of activity coefficients at infinite dilution of aliphatic and aromatic hydrocarbons, alcohols, thiophene, tetrahydrofuran, MTBE, and water in ionic liquid [BMIM][SCN] using GLC. *J Chem Thermodyn* 2009;41(5):645–50.

[26] Domańska U, Marciniak A. Measurements of activity coefficients at infinite dilution of aromatic and aliphatic hydrocarbons, alcohols, and water in the new ionic liquid [EMIM][SCN] using GLC. *J Chem Thermodyn* 2008;40(5):860–6.

[27] Domanska U, Marciniak A. Activity coefficients at infinite dilution measurements for organic solutes and water in the ionic liquid 1-butyl-3-methylimidazolium trifluoromethanesulfonate. *J Phys Chem B* 2008;112(35):11100–5.

[28] Domańska U, Marciniak A. Activity coefficients at infinite dilution measurements for organic solutes and water in the ionic liquid triethylsulphonium bis (trifluoromethylsulfonyl) imide. *J Chem Thermodyn* 2009;41(6):754–8.

[29] Domańska U, Paduszyński K. Gas–liquid chromatography measurements of activity coefficients at infinite dilution of various organic solutes and water in tri-iso-butylmethylphosphonium tosylate ionic liquid. *J Chem Thermodyn* 2010;42(6):707–11.

[30] Tumba, K., Reddy, P., Naidoo, P., & Ramjugernath, D. (2011). Activity coefficients at infinite dilution of organic solutes in the ionic liquid trihexyl (tetradecyl) phosphonium tetrafluoroborate using gas–liquid chromatography at T=(313.15, 333.15, 353.15, and 373.15) K. *The Journal of Chemical Thermodynamics*, *43*(5), 670-676.

[31] Tumba K, Letcher T, Naidoo P, Ramjugernath D. Activity coefficients at infinite dilution of organic solutes in the ionic liquid trihexyltetradecylphosphonium hexafluorophosphate using gas–liquid chromatography at T=(313.15, 333.15, 353.15, and 363.15) K. *J Chem Thermodyn* 2012;49:46–53.

[32] Domańska U, Marciniak A. Physicochemical properties and activity coefficients at infinite dilution for organic solutes and water in the ionic liquid 1-decyl-3-methylimidazolium tetracyanoborate. *J Phys Chem B* 2010;114(49):16542–7.

[33] Domańska U, Królikowska M, Acree Jr WE, Baker GA. Activity coefficients at infinite dilution measurements for organic solutes and water in the ionic liquid 1-ethyl-3-methylimidazolium tetracyanoborate. *J Chem Thermodyn* 2011;43(7):1050–7.

[34] Duan JD, Wang LS, Jiang K, Wang XX. Activity coefficients at infinite dilution of organic solutes in 1-octyl-3-methylimidazolium nitrate using gas–liquid chromatography. *Fluid Phase Equilib* 2012;328:1–8.

[35] Feng YX, Wang LS, Li Y. Activity coefficients at infinite dilution of organic solutes in 1-butyl-3-methylimidazolium nitrate using gas– liquid chromatography. *J Chem Eng Data* 2011;56(5):2730–6.

[36] Li Y, Wang LS, Zhang Y. Activity coefficients at infinite dilution of polar solutes in 1-(2-hydroxyethyl)-3-methylimidazolium tetrafluoroborate using gas– liquid chromatography. *J Chem Eng Data* 2010;55(4):1732–4.

[37] Marciniak A. Activity coefficients at infinite dilution and physicochemical properties for organic solutes and water in the ionic liquid 1-(3-hydroxypropyl) pyridinium bis (trifluoromethylsulfonyl)-amide. *J Chem Thermodyn* 2011;43(10):1446–52.

[38] Chen JY, Jiang HX, Liu JL, Jia HX, Jiao YH, Ge ML, et al. Thermodynamics and activity coefficients at infinite dilution for organic compounds and water in the ionic liquid 1-butyl-3-methylimidazolium perchlorate. *J Chem Thermodyn* 2017;115:12–8.

[39] Deenadayalu N, Thango SH, Letcher TM, Ramjugernath D. Measurement of activity coefficients at infinite dilution using polar and non-polar solutes in the ionic liquid 1-methyl-3-octyl-imidazolium diethyleneglycolmonomethylethersulfate at T=(288.15, 298.15, and 313.15) K. *J Chem Thermodyn* 2006;38(5):542–6.

[40] Domańska U, Karpińska M. The use of ionic liquids for separation of binary hydrocarbons mixtures based on gamma infinity data measurements. *J Chem Thermodyn* 2018;127:95–105.

[41] Domańska U, Królikowski M. Measurements of activity coefficients at infinite dilution for organic solutes and water in the ionic liquid 1-ethyl-3-methylimidazolium methanesulfonate. *J Chem Thermodyn* 2012;54:20–7.

[42] Domańska U, Lukoshko EV. Measurements of activity coefficients at infinite dilution for organic solutes and water in the ionic liquid 1-butyl-1-methylpyrrolidinium tricyanomethanide. *J Chem Thermodyn* 2013;66:144–50.

[43] Domańska U, Paduszyński K. *J Chem Thermodyn* 2010;42(11):1361–6.

[44] Domańska U, Wlazło M. Thermodynamics and limiting activity coefficients measurements for organic solutes and water in the ionic liquid 1-dodecyl-3-methylimidzolium bis (trifluoromethylsulfonyl) imide. *J Chem Thermodyn* 2016;103:76–85.

[45] Domańska U, Królikowski M, Acree Jr WE. Thermodynamics and activity coefficients at infinite dilution measurements for organic solutes and water in the ionic liquid 1-butyl-1-methylpyrrolidinium tetracyanoborate. *J Chem Thermodyn* 2011;43(12):1810–7.

[46] Domańska U, Lukoshko EV, Wlazło M. Measurements of activity coefficients at infinite dilution for organic solutes and water in the ionic liquid 1-hexyl-3-methylimidazolium tetracyanoborate. *J Chem Thermodyn* 2012;47:389–96.

[47] Domańska U, Lukoshko EV, Królikowski M. Measurements of activity coefficients at infinite dilution for organic solutes and water in the ionic liquid 1-butyl-1-methylpyrrolidinium tris (pentafluoroethyl) trifluorophosphate ([BMPYR][FAP]). *Chem Eng J* 2012;183:261–70.

[48] Domańska U, Papis P, Szydłowski J. Thermodynamics and activity coefficients at infinite dilution for organic solutes, water and diols in the ionic liquid choline bis (trifluoromethylsulfonyl) imide. *J Chem Thermodyn* 2014;77:63–70.

[49] Domańska U, Karpińska M, Zawadzki M. Activity coefficients at infinite dilution for organic solutes and water in 1-ethyl-1-methylpyrrolidinium lactate. *J Chem Thermodyn* 2015;89:127–33.

[50] Domańska U, Wlazło M, Karpińska M. Activity coefficients at infinite dilution of organic solvents and water in 1-butyl-3-methylimidazolium dicyanamide. A literature review of hexane/hex-1-ene separation. *Fluid Phase Equilib* 2016;417:50–61.

[51] Domańska U, Wlazło M, Karpińska M, Zawadzki M. Separation of binary mixtures hexane/hex-1-ene, cyclohexane/cyclohexene and ethylbenzene/styrene based on limiting activity coefficients. *J Chem Thermodyn* 2017;110:227–36.

[52] Domańska U, Karpińska M, Wlazło M. Thermodynamic study of molecular interaction-selectivity in separation processes based on limiting activity coefficients. *J Chem Thermodyn* 2018;121:112–20.

[53] Domańska U, Wlazło M, Karpińska M, Zawadzki M. New ionic liquid [P4, 4, 4, 4][NTf2] in bio-butanol extraction on investigation of limiting activity coefficients. *Fluid Phase Equilib* 2018;475:89–94.

[54] Domínguez I, Gonzalez B, Orge B, Held C, Voges M, Macedo EA. Activity coefficients at infinite dilution for different alcohols and ketones in [EMpy][ESO4]: Experimental data and modeling with PC-SAFT. *Fluid Phase Equilib* 2016;424:32–40.

[55] Ge ML, Wang LS. Activity coefficients at infinite dilution of polar solutes in 1-butyl-3-methylimidazolium trifluoromethanesulfonate using gas–liquid chromatography. *J Chem Eng Data* 2008;53(3):846–9.

[56] Hector T, Uhlig L, Gmehling J. Prediction of different thermodynamic properties for systems of alcohols and sulfate-based anion Ionic Liquids using modified UNIFAC. *Fluid Phase Equilib* 2013;338:135–40.

[57] Karpińska M, Wlazło M, Domańska U. Separation of binary mixtures based on gamma infinity data using [EMIM][TCM] ionic liquid and modelling of thermodynamic functions. *J Mol Liq* 2017;225:382–90.

[58] Karpińska M, Wlazło M, Zawadzki M, Domańska U. Separation of binary mixtures hexane/hex-1-ene, cyclohexane/cyclohexene and ethylbenzene/styrene based on gamma infinity data measurements. *J Chem Thermodyn* 2018;118:244–54.

[59] Lukoshko E, Mutelet F, Domanska U. Experimental and theoretically study of interaction between organic compounds and tricyanomethanide based ionic liquids. *J Chem Thermodyn* 2015;85:49–56.

[60] Marciniak A, Wlazło M. Activity coefficients at infinite dilution and physicochemical properties for organic solutes and water in the ionic liquid 1-(2-methoxyethyl)-1-methylpyrrolidinium bis(trifluoromethylsulfonyl)-amide. J Chem Thermodyn 2012;54:90–6.

[61] Marciniak A, Wlazło M. Activity coefficients at infinite dilution and physicochemical properties for organic solutes and water in the ionic liquid 4-(2-methoxyethyl)-4-methylmorpholinium bis (trifluoromethylsulfonyl)-amide. *J Chem Thermodyn* 2012;47:382–8.

[62] Marciniak A, Wlazło M. Activity coefficients at infinite dilution and physicochemical properties for organic solutes and water in the ionic liquid 1-(2-methoxyethyl)-1-methylpiperidinium bis (trifluoromethylsulfonyl)-amide. *J Chem Thermodyn* 2012;49:137–45.

[63] Marciniak A, Wlazło M. Activity coefficients at infinite dilution and physicochemical properties for organic solutes and water in the ionic liquid 1-(2-methoxyethyl)-1-methylpiperidinium trifluorotris (perfluoroethyl) phosphate. *J Chem Thermodyn* 2013;57:197–202.

[64] Marciniak A, Wlazło M. Activity coefficients at infinite dilution and physicochemical properties for organic solutes and water in the ionic liquid 1-(2-hydroxyethyl)-3-methylimidazolium trifluorotris (perfluoroethyl) phosphate. *J Chem Thermodyn* 2013;64:114–9.

[65] Marciniak A, Wlazło M. Activity coefficients at infinite dilution and physicochemical properties for organic solutes and water in the ionic liquid 1-(2-methoxyethyl)-1-methylpyrrolidinium trifluorotris (perfluoroethyl) phosphate. *J Chem Thermodyn* 2013;60:57–62.

[66] Marciniak A, Wlazło M. Activity coefficients at infinite dilution, physicochemical and thermodynamic properties for organic solutes and water in the ionic liquid ethyl-dimethyl-(2-methoxyethyl) ammonium trifluorotris-(perfluoroethyl) phosphate. *J Chem Thermodyn* 2015;89:245–50.

[67] Marsh KN, Brennecke JF, Chirico RD, Frenkel M, Heintz A, Magee JW, et al. Thermodynamic and thermophysical properties of the reference ionic liquid: 1-Hexyl-3-methylimidazolium bis [(trifluoromethyl) sulfonyl] amide (including mixtures). Part 1. Experimental methods and results (IUPAC Technical Report). *Pure Appl Chem* 2009;81(5):781–90.

[68] Mutelet F, Alonso D, Ravula S, Baker GA, Jiang B, Acree Jr WE. Infinite dilution activity coefficients of solutes dissolved in anhydrous alkyl (dimethyl) isopropylammonium bis (trifluoromethylsulfonyl) imide ionic liquids containing functionalized-and nonfunctionalized-alkyl chains. *J Mol Liq* 2016;222:295–312.

[69] Olivier E, Letcher TM, Naidoo P, Ramjugernath D. Activity coefficients at infinite dilution of organic solutes in the ionic liquid 1-octyl-3-methylimidazolium hexafluorophosphate using gas–liquid chromatography at T=(313.15, 323.15, and 333.15) K. *J Chem Thermodyn* 2010;42(5):646–50.

[70] Paduszynski K, Domanska U. Limiting activity coefficients and gas–liquid partition coefficients of various solutes in piperidinium ionic liquids: measurements and LSER calculations. *J Phys Chem B* 2011;115(25):8207–15.

[71] Paduszyński K, Domańska U. Experimental and theoretical study on infinite dilution activity coefficients of various solutes in piperidinium ionic liquids. *J Chem Thermodyn* 2013;60:169–78.

[72] Rabhi F, Hussard C, Sifaoui H, Mutelet F. Characterization of bis (fluorosulfonyl) imide based ionic liquids by gas chromatography. *J Mol Liq* 2019;289:111169.

[73] Vilas-Boas SM, Teixeira G, Rosini S, Martins MA, Gaschi PS, Coutinho JA, et al. Ionic liquids as entrainers for terpenes fractionation and other relevant separation problems. *J Mol Liq* 2021;323:114647.

[74] Wlazło M, Marciniak A. Activity coefficients at infinite dilution and physicochemical properties for organic solutes and water in the ionic liquid 4-(2-methoxyethyl)-4-methylmorpholinium trifluorotris (perfluoroethyl) phosphate. *J Chem Thermodyn* 2012;54:366–72.

[75] Wlazło M, Marciniak A, Letcher TM. Activity coefficients at infinite dilution and physicochemical properties for organic solutes and water in the ionic liquid 1-ethyl-3-methylimidazolium trifluorotris (perfluoroethyl) phosphate. *J Solution Chem* 2015;44:413–30.

[76] Wlazło M, Marciniak A, Zawadzki M, Dudkiewicz B. Activity coefficients at infinite dilution and physicochemical properties for organic solutes and water in the ionic liquid 4-(3-hydroxypropyl)-4-methylmorpholinium bis (trifluoromethylsulfonyl)-amide. *J Chem Thermodyn* 2015;86:154–61.

[77] Wlazło M, Zawadzki M, Domańska U. Separation of water/butan-1-ol based on activity coefficients at infinite dilution in 1, 3-didecyl-2-methylimidazolium dicyanamide ionic liquid. *J Chem Thermodyn* 2018;116:316–22.

[78] Yan PF, Liu QS, Yang M, Liu XM, Tan ZC, Welz-Biermann U. Activity coefficients at infinite dilution of organic solutes in N-alkylpyridinium bis (trifluoromethylsulfonyl) imide ([CnPY][NTf2], n= 2, 4, 5) using gas–liquid chromatography. *J Chem Thermodyn* 2010;42(12):1415–22.

[79] Zhang M, He ZZ, Kang RX, Ge ML. Thermodynamics and activity coefficients at infinite dilution for organic compounds in the ionic liquid 1-hexyl-3-methylimidazolium chloride. *J Chem Thermodyn* 2019;128:187–94.

[80] Zhang C, Triger D, Ramer NJ. Activity coefficients at infinite dilution for various organic solutes in the ionic liquid 1-(2-hydroxyethyl)-3-methylimidazolium hexafluorophosphate. *J Chem Thermodyn* 2020;140:105867.

[81] Zhang T, Bao YN, Zhang L, Ren RZ, Jiao YH, Ge ML. Thermodynamics and selectivity of separation based on activity coefficients at infinite dilution of various solutes in ionic liquid [DMIM][Tf2N]. *J Chem Thermodyn* 2020;147:106120.

[82] Ayad A, Mutelet F, Negadi A, Acree Jr WE, Jiang B, Lu A, et al. Activity coefficients at infinite dilution for organic solutes dissolved in two 1-alkylquinuclidinium bis (trifluoromethylsulfonyl) imides bearing alkyl side chains of six and eight carbons. *J Mol Liq* 2016;215:176–84.

[83] Blahut A, Dohnal V. Interactions of volatile organic compounds with the ionic liquid 1-butyl-1-methylpyrrolidinium dicyanamide. *J Chem Eng Data* 2011;56(12):4909–18.

[84] Blahut A, Dohnal V. Interactions of volatile organic compounds with the ionic liquids 1-butyl-1-methylpyrrolidinium tetracyanoborate and 1-butyl-1-methylpyrrolidinium bis (oxalato) borate. *J Chem Thermodyn* 2013;57:344–54.

[85] Blahut A, Sobota M, Dohnal V, Vrbka P. Activity coefficients at infinite dilution of organic solutes in the ionic liquid 1-ethyl-3-methylimidazolium methanesulfonate. *Fluid Phase Equilib* 2010;299(2):198–206.

[86] Blahut A, Dohnal V, Vrbka P. Interactions of volatile organic compounds with the ionic liquid 1-ethyl-3-methylimidazolium tetracyanoborate. *J Chem Thermodyn* 2012;47:100–8.

[87] Deenadayalu N, Letcher TM, Reddy P. Determination of activity coefficients at infinite dilution of polar and nonpolar solutes in the ionic liquid 1-ethyl-3-methylimidazolium bis (trifluoromethylsulfonyl) imidate using gas− liquid chromatography at the temperature 303.15 K or 318.15 K. *J Chem Eng Data* 2005;50(1):105–8.

[88] Domanska U, Królikowska M. Measurements of activity coefficients at infinite dilution for organic solutes and water in the ionic liquid 1-butyl-1-methylpiperidinium thiocyanate. *J Chem Eng Data* 2011;56(1):124–9.

[89] Domańska U, Zawadzki M, Królikowska M, Tshibangu MM, Ramjugernath D, Letcher TM. Measurements of activity coefficients at infinite dilution of organic compounds and water in isoquinolinium-based ionic liquid [C8iQuin][NTf2] using GLC. *J Chem Thermodyn* 2011;43(3):499–504.

[90] Durski M, Naidoo P, Ramjugernath D, Domańska U. Thermodynamics and activity coefficients at infinite dilution for organic solutes in the ionic liquid 1-butyl-1-methylpyrrolidinium dicyanamide. *Fluid Phase Equilib* 2018;473:175–82.

[91] Królikowska M, Karpińska M, Królikowski M. Measurements of activity coefficients at infinite dilution for organic solutes and water in N-hexylisoquinolinium thiocyanate,[HiQuin][SCN] using GLC. *J Chem Thermodyn* 2013;62:1–7.

[92] Królikowski M, Królikowska M, Markowski C. The investigation of the infinite dilution activity coefficients for molecular compounds in 1-(3-hydroxypropyl)-3-methyl-imidazolium thiocyanate. *J Chem Thermodyn* 2021;161:106554.

[93] Li J, Wang Q, Tian L, Li Z, Li Y, Hu Y, et al. Application potential of N-hexylpyridinium bromide for separation azeotrope: Thermodynamic properties measurements. *Fluid Phase Equilib* 2022;557:113436.

[94] Marciniak A, Wlazlo M. Activity coefficients at infinite dilution measurements for organic solutes and water in the ionic liquid 1-butyl-3-methyl-pyridinium trifluoromethanesulfonate. *J Chem Eng Data* 2010;55(9):3208–11.

[95] Órfão EF, Dohnal V, Blahut A. Infinite dilution activity coefficients of volatile organic compounds in two ionic liquids composed of the tris (pentafluoroethyl) trifluorophosphate ([FAP]) anion and a functionalized cation. *J Chem Thermodyn* 2013;65:53–64.

[96] Paduszyński K, Królikowska M. Interactions between molecular solutes and task-specific ionic liquid: Measurements of infinite dilution activity coefficients and modeling. *J Mol Liq* 2016;221:235–44.

[97] Shida T, Hiraga Y, Sugiyama T, Sato Y, Watanabe M, Smith Jr RL. Measurement and modeling of infinite dilution activity coefficients of organic compounds in an equimolar ionic liquid mixture of [Bmim] Cl and [Bmim][Tf2N]. *Fluid Phase Equilib* 2019;488:72–8.

[98] Sobota M, Dohnal V, Vrbka P. Activity coefficients at infinite dilution of organic solutes in the ionic liquid 1-ethyl-3-methyl-imidazolium nitrate. *J Phys Chem B* 2009;113(13):4323–32.

[99] Stark A, Ondruschka B, Zaitsau DH, Verevkin SP. Biomass-derived platform chemicals: thermodynamic studies on the extraction of 5-hydroxymethylfurfural from ionic liquids. *J Chem Eng Data* 2012;57(11):2985–91.

[100] Sumartschenkowa IA, Verevkin SP, Vasiltsova TV, Bich E, Heintz A, Shevelyova MP, et al. Experimental Study of Thermodynamic Properties of Mixtures Containing Ionic Liquid 1-Ethyl-3-methylimidazolium Ethyl Sulfate Using Gas− Liquid Chromatography and Transpiration Method. *J Chem Eng Data* 2006;51(6):2138–44.

[101] Yan PF, Yang M, Liu XM, Liu QS, Tan ZC, Welz-Biermann U. Activity Coefficients at Infinite Dilution of Organic Solutes in 1-Ethyl-3-methylimidazolium Tris (pentafluoroethyl) trifluorophosphate [EMIM][FAP] Using Gas− Liquid Chromatography. *J Chem Eng Data* 2010;55(7):2444–50.

[102] Yan PF, Yang M, Liu XM, Wang C, Tan ZC, Welz-Biermann U. Activity coefficients at infinite dilution of organic solutes in the ionic liquid 1-ethyl-3-methylimidazolium tetracyanoborate [EMIM][TCB] using gas–liquid chromatography. *J Chem Thermodyn* 2010;42(6):817–22.

[103] Yan PF, Yang M, Li CP, Liu XM, Tan ZC, Welz-Biermann U. Gas-liquid chromatography measurements of activity coefficients at infinite dilution of hydrocarbons and alkanols in 1-alkyl-3-methylimidazolium bis (oxalato) borate. *Fluid Phase Equilib* 2010;298(2):287–92.

[104] Zhang M, Ge ML, Jiao YH, Mu Z, Huang R, He ZZ. Determination of the thermodynamic parameters of ionic liquid 1-propyl-3-methylimidazolium bromide by gas-liquid chromatography. *J Chem Thermodyn* 2019;129:92–8.

[105] Zhou Q, Wang LS, Wu JS, Li MY. Activity coefficients at infinite dilution of polar solutes in 1-Butyl-3-methylimidazolium tetrafluoroborate using gas− liquid chromatography. *J Chem Eng Data* 2007;52(1):131–4.

[106] Bahadur I, Govender BB, Osman K, Williams-Wynn MD, Nelson WM, Naidoo P, et al. Measurement of activity coefficients at infinite dilution of organic solutes in the ionic liquid 1-ethyl-3-methylimidazolium 2-(2-methoxyethoxy) ethylsulfate at T=(308.15, 313.15, 323.15 and 333.15) K using gas+ liquid chromatography. *J Chem Thermodyn* 2014;70:245–52.

[107] Bahadur I, Naidoo M, Naidoo P, Ramdath S, Ramjugernath D, Ebenso EE. Screening of environmental friendly ionic liquid as a solvent for the different types of separations problem: Insight from activity coefficients at infinite dilution measurement using (gas+ liquid) chromatography technique. *J Chem Thermodyn* 2016;92:35–42.

[108] Deng L, Wang Q, Chen Y, Zhang Z, Tang J. Determination of the solubility parameter of ionic liquid 1-octyl-3-methylimidazolium hexafluorophosphate by inverse gas chromatography. *J Mol Liq* 2013;187:246–51.

[109] Heintz A, Kulikov DV, Verevkin SP. Thermodynamic properties of mixtures containing ionic liquids. Activity coefficients at infinite dilution of polar solutes in 4-methyl-N-butyl-pyridinium tetrafluoroborate using gas–liquid chromatography. *J Chem Thermodyn* 2002;34(8):1341–7.

[110] Heintz A, Kulikov DV, Verevkin SP. Thermodynamic properties of mixtures containing ionic liquids. 2. Activity coefficients at infinite dilution of hydrocarbons and polar solutes in 1-methyl-3-ethyl-imidazolium bis (trifluoromethyl-sulfonyl) amide and in 1, 2-dimethyl-3-ethyl-imidazolium bis (trifluoromethyl-sulfonyl) amide using gas− liquid chromatography. *J Chem Eng Data* 2002;47(4):894–9.

[111] Heintz A, Vasiltsova TV, Safarov J, Bich E, Verevkin SP. Thermodynamic properties of mixtures containing ionic liquids. 9. Activity coefficients at infinite dilution of hydrocarbons, alcohols, esters, and aldehydes in trimethyl-butylammonium bis (trifluoromethylsulfonyl) imide using gas− liquid chromatography and static method. *J Chem Eng Data* 2006;51(2):648–55.

[112] Kabane B, Redhi GG. Application of trihexyltetradecylphosphonium dicyanamide ionic liquid for various types of separations problems: Activity coefficients at infinite dilution measurements utilizing GLC method. *Fluid Phase Equilib* 2019;493:181–7.

[113] Kabane B, Chokkareddy R, Redhi GG. Separation of (water/butan-1-ol) binary systems based on activity coefficients at infinite dilution with phosphonium ionic liquid. *J Chem Thermodyn* 2019;137:7–12.

[114] Kato R, Gmehling J. Activity coefficients at infinite dilution of various solutes in the ionic liquids [MMIM]+[CH3SO4]−,[MMIM]+[CH3OC2H4SO4]−,[MMIM]+[(CH3) 2PO4]−,[C5H5NC2H5]+[(CF3SO2) 2N]− and [C5H5NH]+[C2H5OC2H4OSO3]−. *Fluid Phase Equilib* 2004;226:37–44.

[115] Kato R, Gmehling J. Systems with ionic liquids: Measurement of VLE and γ∞ data and prediction of their thermodynamic behavior using original UNIFAC, mod. UNIFAC (Do) and COSMO-RS (Ol). *J Chem Thermodyn* 2005;37(6):603–19.

[116] Królikowski M, Królikowska M, Więckowski M, Piłowski A. The influence of the ionic liquids functionalization on interaction in binary systems with organic solutes and water–Thermodynamic data of activity coefficients at infinite dilution. *J Chem Thermodyn* 2020;147:106117.

[117] Krummen M, Wasserscheid P, Gmehling J. Measurement of activity coefficients at infinite dilution in ionic liquids using the dilutor technique. *J Chem Eng Data* 2002;47(6):1411–7.

[118] Letcher, T. M., Ramjugernath, D., Laskowska, M., Królikowski, M., Naidoo, P., & Domańska, U. (2008). Determination of activity coefficients at infinite dilution of solutes in the ionic liquid, trihexyltetradecylphosphonium bis (trifluoromethylsulfonyl) imide, using gas− liquid chromatography at T= (303.15, 308.15, 313.15, and 318.15) K. *Journal of Chemical & Engineering Data*, *53*(9), 2044-2049.

[119] Martins MA, Coutinho JA, Pinho SP, Domańska U. Measurements of activity coefficients at infinite dilution of organic solutes and water on polar imidazolium-based ionic liquids. *J Chem Thermodyn* 2015;91:194–203.

[120] Martins MA, Vilas-Boas SM, Cordova IW, Carvalho PJ, Domańska U, Ferreira O, et al. Infinite Dilution Activity Coefficients in the Smectic and Isotropic Phases of Tetrafluoroborate-Based Ionic Liquids. *J Chem Eng Data* 2021;66(6):2587–96.

[121] Paduszyński K, Królikowski M. An effect of cation's cyano group on interactions between organic solutes and ionic liquids elucidated by thermodynamic data at infinite dilution. *J Mol Liq* 2017;243:726–36.

[122] Revelli AL, Mutelet F, Turmine M, Solimando R, Jaubert JN. Activity coefficients at infinite dilution of organic compounds in 1-butyl-3-methylimidazolium tetrafluoroborate using inverse gas chromatography. *J Chem Eng Data* 2009;54(1): 90–101.

[123] Tian L, Chen Y, Wang Q. Yingyong Huaxue 2014;34(7):824.

[124] Tumba K, Letcher TM, Naidoo P, Ramjugernath D. Activity coefficients at infinite dilution of organic solutes in the ionic liquid trihexyltetradecylphosphonium bis (trifluoromethylsulfonyl) imide using gas–liquid chromatography at T=(313.15, 333.15, 353.15 and 373.15) K. *J Chem Thermodyn* 2013;65:159–67.

[125] Vasil'tsova TV, Heintz A, Kulikov D, Verevkin SP. Kholod Tekh Tekhnol 2003;84 (4):49.

[126] Ziemblińska-Bernart J, Bielecki P, Wasiak W. Measurements of activity coefficients at infinite dilution for organic solutes in two quaternary ammonium-based ionic liquids [DDA][ClO4] and [DDA][BF4]. *Fluid Phase Equilib* 2019;482: 99–107.

[127] Acree Jr WE, Baker GA, Mutelet F, Moise JC. Partition coefficients of organic compounds in four new tetraalkylammonium bis (trifluoromethylsulfonyl) imide ionic liquids using inverse gas chromatography. *J Chem Eng Data* 2011;56(9): 3688–97.

[128] Banerjee T, Khanna A. Infinite dilution activity coefficients for trihexyltetradecyl phosphonium ionic liquids: measurements and COSMO-RS prediction. *J Chem Eng Data* 2006;51(6):2170–7.

[129] Foco GM, Bottini SB, Quezada N, de la Fuente JC, Peters CJ. Activity coefficients at infinite dilution in 1-alkyl-3-methylimidazolium tetrafluoroborate ionic liquids. *J Chem Eng Data* 2006;51(3):1088–91.

[130] Letcher TM, Reddy P. Determination of activity coefficients at infinite dilution of organic solutes in the ionic liquid, trihexyl (tetradecyl)-phosphonium tris (pentafluoroethyl) trifluorophosphate, by gas–liquid chromatography. *Fluid Phase Equilib* 2005;235(1):11–7.

[131] Letcher TM, Soko B, Ramjugernath D, Deenadayalu N, Nevines A, Naicker PK. Activity coefficients at infinite dilution of organic solutes in 1-hexyl-3-methyli-midazolium hexafluorophosphate from gas− liquid chromatography. *J Chem Eng Data* 2003;48(3):708–11.

[132] Letcher TM, Marciniak A, Marciniak M, Domańska U. Determination of activity coefficients at infinite dilution of solutes in the ionic liquid 1-butyl-3-methyli-midazolium octyl sulfate using gas− liquid chromatography at a temperature of 298.15 K, 313.15 K, or 328.15 K. *J Chem Eng Data* 2005;50(4):1294–8.

[133] Letcher TM, Domańska U, Marciniak M, Marciniak A. Activity coefficients at infinite dilution measurements for organic solutes in the ionic liquid 1-butyl-3-methyl-imidazolium 2-(2-methoxyethoxy) ethyl sulfate using glc at T=(298.15, 303.15, and 308.15) K. *J Chem Thermodyn* 2005;37(6):587–93.

[134] Moïse JC, Mutelet F, Jaubert JN, Grubbs LM, Acree Jr WE, Baker GA. Activity coefficients at infinite dilution of organic compounds in four new imidazolium-based ionic liquids. *J Chem Eng Data* 2011;56(7):3106–14.

[135] Mutelet F, Revelli AL, Jaubert JN, Sprunger LM, Acree Jr WE, Baker GA. Partition coefficients of organic compounds in new imidazolium and tetralkylammonium based ionic liquids using inverse gas chromatography. *J Chem Eng Data* 2010;55 (1):234–42.

[136] Mutelet F, Hassan ESR, Stephens TW, Acree Jr WE, Baker GA. Activity coefficients at infinite dilution for organic solutes dissolved in three 1-alkyl-1-methylpyrro-lidinium bis (trifluoromethylsulfonyl) imide ionic liquids bearing short linear alkyl side chains of three to five carbons. *J Chem Eng Data* 2013;58(8):2210–8.

[137] Olivier E, Letcher TM, Naidoo P, Ramjugernath D. Activity coefficients at infinite dilution of organic solutes in the ionic liquid 1-ethyl-3-methylimidazolium trifluoromethanesulfonate using gas–liquid chromatography at T=(313.15, 323.15, and 333.15) K. *J Chem Thermodyn* 2010;42(1):78–83.

[138] Diedenhofen M, Eckert F, Klamt A. Prediction of infinite dilution activity coefficients of organic compounds in ionic liquids using COSMO-RS. *J Chem Eng Data* 2003;48(3):475–9.

[139] Klamt A. Conductor-like screening model for real solvents: a new approach to the quantitative calculation of solvation phenomena. J Phys Chem 1995;99(7): 2224–35.

[140] Klamt A, Jonas V, Bürger T, Lohrenz JC. Refinement and parametrization of COSMO-RS. Chem A Eur J 1998;102(26):5074–85.

[141] Eckert F, Klamt A. Fast solvent screening via quantum chemistry: COSMO-RS approach. AIChE J 2002;48(2):369–85.

[142] BIOVIA COSMOtherm, Release 2023; Dassault Systèmes. http://www.3ds.com.

[143] Modarresi H, Modarress H, Dearden JC. QSPR model of Henry's law constant for a diverse set of organic chemicals based on genetic algorithm-radial basis function network approach. *Chemosphere* 2007;66(11):2067–76.

[144] Shahlaei M. Descriptor selection methods in quantitative structure–activity relationship studies: a review study. *Chem Rev* 2013;113(10):8093–103.

[145] Khooshechin S, Dashtbozorgi Z, Golmohammadi H, Acree Jr WE. QSPR prediction of gas-to-ionic liquid partition coefficient of organic solutes dissolved in 1-(2-hydroxyethyl)-1-methylimidazolium tris (pentafluoroethyl) trifluorophosphate using the replacement method and support vector regression. *J Mol Liq* 2014;196: 43–51.

[146] Holland JH. Adaption in natural and artificial systems. Ann Arbor MI: The University of MichiganPress; 1975.

[147] New Jersey: Hoboken; 2004.

[148] Lemaoui T, Darwish AS, Hammoudi NEH, Abu Hatab F, Attoui A, Alnashef IM, et al. Prediction of electrical conductivity of deep eutectic solvents using COSMO-RS sigma profiles as molecular descriptors: a quantitative structure–property relationship study. *Ind Eng Chem Res* 2020;59(29):13343–54.

[149] Ojha PK, Roy K. Comparative QSARs for antimalarial endochins: importance of descriptor-thinning and noise reduction prior to feature selection. *Chemom Intel Lab Syst* 2011;109(2):146–61.

[150] He W, Yan F, Jia Q, Xia S, Wang Q. Description of the thermal conductivity λ (T, P) of ionic liquids using the structure–property relationship method. *J Chem Eng Data* 2017;62(8):2466–72.

[151] Amini Z, Fatemi MH, Gharaghani S. Hybrid docking-QSAR studies of DPP-IV inhibition activities of a series of aminomethyl-piperidones. *Comput Biol Chem* 2016;64:335–45.

[152] Liu X, Yu M, Jia Q, Yan F, Zhou YN, Wang Q. Leave-one-ion-out cross-validation for assisting in developing robust QSPR models of ionic liquids. *J Mol Liq* 2023; 388:122711.

[153] Makarov DM, Fadeeva YA, Shmukler LE, Tetko IV. Beware of proper validation of models for ionic Liquids! *J Mol Liq* 2021;344:117722.